Telecommunication Systems (2024) 85:563–590
https://doi.org/10.1007/s11235-024-01101-0

Maximizing throughput and energy efficiency in 6G based on phone user clustering enabled UAV assisted downlink hybrid multiple access HetNet

Umar Ghafoor[1] · **Tahreem Ashraf**[2]

Accepted: 1 January 2024 / Published online: 13 February 2024

Abstract
The surge in technology is driving demands for real-time interactive applications and high-speed transmissions, necessitating improved network throughput and energy efficiency (EE) for immersive experiences. The rise in industrial automation has led to higher connectivity needs, straining fifth-generation networks. Sixth-generation networks aim to address these demands, potentially maximizing throughput and EE through enhanced coverage. This paper introduces innovative techniques like phone user clustering-based downlink hybrid multiple access in unmanned aerial vehicle-assisted heterogeneous networks (HetNets) to jointly optimize phone user (PU) admission, cell association, throughput, and EE while ensuring PU fair association with cell (PUFAC) and quality of service (QoS), i.e., minimum rate requirement of PUs. An outer approximation algorithm solves the mixed integer non-linear programming (MINLP) optimization problem arising from the transformation of the concave fractional programming optimization problem using the Charnes-Cooper transformation. The method's effectiveness is assessed, showcasing its superiority over existing macro-cell-only networks and HetNets concerning throughput, EE, PU admission, PU-cell association, PUFAC, and QoS.

Keywords UAV · OMA · NOMA · H-MA · Throughput maximization · EE maximization · 6G · MINLP · OAA

1 Introduction

Over the recent decades, there has been a noteworthy surge in the demand for wireless mobile communication system services, resulting in an upsurge in data rates or throughput and energy utilization within communication infrastructures [1]. This situation has elicited concerns for operators and the ecological surroundings. Predictions indicate a substantial projected escalation, approximately ranging from 150 to 170%, in throughput and energy consumption within the fifth generation (5G) and forthcoming sixth generation (6G) wireless systems by 2026 [2]. Hence, network operators are actively investigating technologies that are adept at reducing energy consumption while augmenting the network throughput [3]. Recent investigations have primarily concentrated on optimizing energy efficiency (EE) to promote sustainability, instigating endeavors to formulate communication networks centered around EE concepts [4, 5]. In this context, throughput and EE are precisely defined as the attainable data rate and the quotient of attainable data rate to power consumption, respectively, with the primary approach being the maximization of network throughput alongside the minimization of energy utilization.

In the domain of wireless networks, the notion of heterogeneous networks (HetNets) has surfaced as a technology capable of augmenting both throughput and EE in contrast to networks comprising exclusively of macro cells (MCs). A characteristic configuration of a HetNet involves integrating a MC with small cell (SC). Exploiting SC within HetNets, which exhibit reduced energy consumption due to their lower power requirement, becomes advantageous. Placing SCs in closer proximity to phone users (PUs) in densely populated areas heightens signal strength, diminishing the dependence on high-power transmissions from distant MCs. Strategically dispersed SC contribute to an overall reduction in power usage by covering smaller areas with diminished power demand [6, 7]. These SCs additionally alleviate traffic congestion from MCs, enabling them to function at decreased

✉ Umar Ghafoor
ch.umar163@gmail.com

[1] National University of Sciences and Technology, Islamabad, Pakistan

[2] Government College University, Faisalabad, Pakistan

power levels and thereby elevating both throughput and EE. Thus, HetNets offer a more energy-conscious approach to network deployment, proficiently utilizing resources and curbing superfluous power consumption when compared to setups reliant solely on MCs [8, 9].

Incorporating unmanned aerial vehicles (UAVs) into HetNets presents an opportunity for even more substantial improvements in throughput and EE. UAVs can be deployed as needed to offer temporary coverage in densely populated or remote regions, providing targeted service without continuous power consumption. Functioning as aerial base stations, UAVs can relieve the load on ground-based cells during peak periods, thus curbing their power usage. Intelligent routing algorithms can optimize the flight paths of UAVs to ensure network connectivity while conserving energy. Additionally, UAVs can serve as mobile backhaul nodes, minimizing the reliance on energy-intensive wired connections and facilitating data relay [10, 11]. The utilization of renewable energy sources such as solar panels to power UAVs can simultaneously diminish the carbon footprint and operational costs. Both ground-based cells and UAVs can employ communication protocols designed for EE, thereby further decreasing energy consumption while upholding service quality. This amalgamation of UAVs and HetNets, coupled with energy-conscious approaches, holds the potential to elevate network throughput and EE, trim operational expenditures, and mitigate environmental repercussions [12].

Effectively allocating limited radio resources among multiple PUs using a range of multiple access (MA) techniques is crucial in the enhancement of throughput and EE within wireless networks. These methods enable numerous PUs to access the same frequency band simultaneously, resulting in improved resource distribution, minimized spectrum wastage, and consequently heightened EE. Proficient management of MA also mitigates interference, lessening the need for elevated transmission power and conserving energy consumption [13]. Hybrid MA (H-MA) integrates non-orthogonal MA (NOMA) with orthogonal MA (OMA), offering efficient resource allocation to PUs. It facilitates resource sharing via NOMA while allocating orthogonal resources when required, thereby optimizing resource utilization, particularly in fluctuating channel conditions. H-MA outperforms OMA in EE by capitalizing on the resource-sharing advantages of NOMA while retaining orthogonal channels for specific PUs, harmonizing effectively with dynamic scenarios and ultimately advancing overall EE. As an amalgamation of the strengths of NOMA and OMA, H-MA emerges as a favored solution for energy-efficient wireless communication systems, adept in resource optimization, interference reduction, and adaptability to diverse network conditions [14, 15].

PU clustering, known as PUC, emerges as a pivotal strategy for the optimization of both throughput and EE in wireless communication systems. This methodology entails the grouping of PUs based on factors such as proximity, channel conditions, or traffic patterns. Through the clustering of PUs exhibiting similar attributes, the network gains the capability to finely calibrate resource allocation, ensuring the efficient utilization of radio spectrum, power, and network resources to curtail wastage while maximizing throughput and EE [16]. These clusters reap the benefits of shared channel conditions, which in turn diminish interference and decrease the energy demand for reliable communication. PUC also accomplishes the equitable distribution of traffic across the network; during instances of heightened demand within a cluster, load balancing diverts PUs to less congested clusters, thereby optimizing energy consumption. PUC fosters cooperative communication within clusters, allowing closely situated PUs to collaborate in information exchange, thereby mitigating transmission power for long-distance communication [17]. On the whole, PUC augments resource management, reduces interference, and nurtures a wireless network marked by enhanced EE, ultimately contributing to elevated throughput, and EE.

1.1 Existing works

This section presents a comprehensive examination of the existing literature, summarizing noteworthy findings and outcomes, which are compiled and presented in Table 1.

The paper [18] focuses on maximizing the cost efficiency subject to the imperfect alignment in millimeterWave (mmWave) NOMA-HetNet. Learning-based Cost-efficient Resource Allocation (LCRA) algorithm is employed to achieve the objective by solving the problem formulated as stochastic combinatorial optimization problem. A fresh perspective combining OMA and HetNet [19] is developed for the allocation and optimization of radio resources. This approach adapts to evolving user quality of experience (QoE) requirements and aims to decrease energy usage by solving the formulated problem as non-convex optimization problem. By utilizing parked cars as roadside units (P-RSUs), [20] establishes cellular-vehicle-to-vehicle HetNets (C-V2V HetNets), thereby fortifying urban vehicular networks. This is succeeded by an optimization framework concentrating on achieving maximal EE in C-V2V OMA based HetNets that involve parked cars. Examining energy harvesting within NOMA HetNets, [21] delves into a combined subchannel and power allocation scheme aimed at heightening the EE of small cells subject to quality of service (QoS) constraint. In [22], a pioneering algorithm called the energy consumption optimization algorithm (ECOA) is introduced, which merges cell selection and OMA assisted HetNet techniques to realize the optimization of energy consumption while maintaining network performance, i.e., QoS at the forefront.

Table 1 Literature review

References	Objective	Constraints	Optimization problem	Solution	PU	MC-only	HetNet	UAV	OMA	NOMA	PUC
[18]	Maximize cost efficiency	Imperfect alignment	Stochastic combinatorial	LCRA	✓		✓			✓	
[19]	Reduce energy consumption	QoE	Non-convex	Heuristic	✓		✓		✓		
[20]	Maximize EE	QoS	MINLP	Heuristic	✓		✓		✓		
[21]	Improve EE	QoS	Non-convex	Heuristic	✓		✓			✓	
[22]	Minimize energy consumption	QoS	Convex	ECOA	✓		✓		✓		
[23]	Minimize avg. energy consumption	Optimal position of UAV	Non-convex	Heuristic	✓	✓		✓	✓		
[24]	EE improve	Maintain UAV identification success	Non-convex	Heuristic	✓	✓		✓	✓		
[25]	Maximize system EE	QoS	Non-convex	Heuristic	✓	✓		✓	✓		
[26]	Minimize energy consumption	Dynamic adjustment of UAV	Non-convex	Heuristic	✓	✓		✓	✓		
[27]	Maximize EE	UAV trajectory	Non-convex	Iterative	✓	✓		✓	✓		
[28]	Maximize outage EE	Energy, transmission power and interference power	Convex	Heuristic	✓	✓		✓	✓		
[29]	EE maximization	QoS	MINLP	Heuristic	✓	✓			✓		
[30]	Minimize energy consumption	Training accuracy	Convex	Heuristic	✓	✓			✓	✓	
[31]	Maximize weighted EE	Total power	Non-convex	SQP	✓	✓				✓	
[32]	Better EE performance	BER	Non-convex	Heuristic	✓	✓				✓	
[33]	Maximize EE	Reduce interference	Non-convex	Heuristic	✓	✓		✓		✓	✓
[34]	EE maximization	QoS	Non-convex	Heuristic	✓	✓				✓	
[35]	EE maximization	Power allocation	Non-convex	Heuristic	✓	✓				✓	
[36]	Enhance sum rate	ISIC	Non-convex	Heuristic	✓	✓			✓	✓	
[37]	Maximize EE	QoS	Non-convex	Geometric programing	✓	✓			✓	✓	
[38]	Maximize EE	QoS	Non-convex	Heuristic	✓	✓			✓		✓
[39]	Maximize EE	QoS	Non-convex	Heuristic	✓	✓			✓		✓
This paper	Maximize rate and EE	PU admission, PU association, QoS, and PUFAC	MINLP	OAA	✓	✓	✓	✓	✓	✓	✓

This work presents various inquiries in the domain of communication networks that benefit from the assistance of UAVs. In [23], a UAV-assisted data collection multi-objective optimization problem (UAVDCMOP) is defined with the objective of minimizing the average energy consumption by refining the positions of UAVs in UAV assisted OMA based MC-only network. The goal is to concurrently elevate the average transmission rate, minimize the total time employed by UAVs, and diminish the average energy consumption of UAVs. In another context, [24] lays out a procedure to identify UAVs that demonstrate energy-efficient traits, while ensuring the achievement of a satisfactory probability of successful UAV identification during the execution of the algorithm in UAV assisted OMA based MC-only network. Addressing a non-convex optimization problem that encompasses subtimeslot allocation and UAV route planning, [25] endeavors to augment the EE of the system subject to QoS requirements of PUs in OMA based UAV assisted MC-only network. Moreover, [26] delves into the effective aggregation of data from machine-type communication devices (MTCDs) through the strategic deployment of UAVs. The approach minimizes overall energy consumption by intricately planning UAV trajectories while accommodating the constraints related to dynamic adjustment of UAVs for the limited energy of both UAVs and MTCDs in OMA based UAV assisted MC-only network. With a deeper focus on UAV EE, [27] puts forth an iterative algorithm that manages PU scheduling and optimizes UAV trajectories to ultimately maximize the EE of UAVs in OMA based UAV assisted MC-only network. In an alternative scenario, [28] explores a setup where UAVs aid in energy harvesting cognitive radio networks (UAV-EH-CRN), assuming the role of cognitive PUs. The objective is to adapt power levels based on outcomes from sensing primary PUs and to actively replenish energy through harvesting, all aimed at optimizing EE during outages while adhering to constraints associated with energy, transmission power, and interference in UAV assisted OMA based MC-only network.

This compilation encompasses a diverse array of investigations within the domain of energy-efficient communication networks. In [29], the focus is on multi-antenna orthogonal frequency division MA (OFDMA) cellular networks, exploring EE and addressing QoS concerns through a formulated mixed integer non-linear programming (MINLP) problem aimed at maximizing EE. In the exploration of edge devices, [30] introduces two transmission protocols for uploading machine learning parameters, employing NOMA and time division MA (TDMA) methodologies. By jointly optimizing variables such as transmission power, rates, and central processing unit (CPU) frequencies, the objective is to minimize overall energy consumption while adhering to training accuracy requirements in MC-only network. Within a NOMA MC-only system, [31] introduces a weighted approach, i.e., sequential quadratic programming (SQP) technique to enhance total weighted EE subject to total power of the system. In [32], a NOMA-based free space optical (FSO) MC-only communication system is compared to an OMA counterpart, showcasing advantages in EE performance. Exploring UAV-assisted full-duplex NOMA technique along with PU clustering (PUC) in MC-only network, [33] addresses EE maximization subject to reduction in interference among PUs, while [34] focuses on a cooperative downlink full-duplex NOMA configuration in the presence of imperfect self-interference cancellation in MC-only network to maximize EE subject to QoS constraint. The impact of hardware limitations on cooperative NOMA technique in MC-only network featuring energy-harvesting relay nodes and intelligent reflecting surfaces is studied in [35], aiming to optimize EE subject to power allocation to PUs. In the proposition of a reconfigurable intelligent surface-assisted hybrid NOMA (H-NOMA) technique in MC-only network in [36], a heuristic approach is explored to enhance the sum rate subject to imperfect successive interference cancellation (ISIC). In [37], EE using random access OMA and NOMA techniques in MC-only network is investigated through mathematical modeling and complementary geometric programming to optimize EE performance.

The increasing energy usage of battery-powered mobile devices, prompted by multimedia applications and growing traffic demands, underscores the significance of EE within mobile ad hoc networks (MANETs). To address this concern, this study introduces a system for optimizing load distribution within MANET clusters, aimed at alleviating energy depletion. The proposed heuristic approach, referred to as HAMBO-CHLD, employs a hybrid algorithm that merges artificial bee colony and monarch butterfly optimization techniques with cluster head load distribution to establish clusters, thereby mitigating energy fatigue in both cluster heads (CHs) and member nodes in PUC assisted OMA based MC-only network [38]. By integrating a weighted clustering parameter, an adaptive clustering strategy is introduced, which incorporates factors such as residual energy, queue length, spectrum availability, and node coverage for the selection of CHs. The CH Weight (CHW) metric guides the CH selection process, followed by an optimal relay selection algorithm based on fuzzy logic (FL) to ensure efficient intra and inter-cluster communication. Parameters like traffic index, link error rate, and channel quality provide inputs to drive the fuzzy system for relay node selection. The proposed heuristic method demonstrates superior performance compared to existing cluster-based routing in sensor networks (CRSN) clustering methods, as substantiated by comprehensive simulation results evaluating residual energy subject to QoS requirement in PUC assisted OMA based MC-only network [39].

1.2 Research gaps and contributions

After an extensive literature review and meticulous examination of the data in Table 1, it becomes clear that the current body of research has yet to produce optimal solutions for effectively tackling the challenges posed by throughput and EE, arising from the disparities in uniformity, diversity, and power allocation between MC and SC in the context of 5G and forthcoming 6G networks. This disparity has instigated a shift in focus for researchers and the academic community, redirecting attention towards the exploration of strategies involving UAVs within HetNet configurations, which are being considered as potential remedies for the intricacies presented by 6G networks. The subsequent sections elaborate on the noteworthy gaps that continue to persist within the ongoing research endeavors, as outlined in Table 2.

It motivates us to joint investigation of all these research gaps. In this paper, we have explored the novel PUC-based downlink H-MA strategy in UAV-assisted HetNet to maximize both throughput and EE regarding performance indicators (PIs). The main contributions of this paper are summarized here in Table 3:

The subsequent sections are organized as follows: Sect. 2 presents the network model and formulates the problem. In Sect. 3, a detailed exposition of the two-stage ϵ-optimal algorithm is presented. Section 4 illustrates the simulation configuration and presents numerical results. Concluding in Sect. 5, the paper summarizes the findings and engages in discussions regarding potential future directions.

2 Network model and problem formulation

A novel approach utilizing PUC-based downlink H-MA is depicted in Fig. 1 for three distinct scenarios: networks comprising solely MC-only network, HetNets, and UAV assisted HetNet. In Fig. 1a, the PUC-based downlink H-MA technique is exemplified in an MC-only network, assuming precise knowledge of channel state information (CSI) at the MC. This scenario accounts for uniformly distributed PUs, enabling PUs to participate in various clusters and affiliate with the MC. Based on the PUs' channel gain values, clusters of PUs are created who are close to each other, optimizing downlink communication for PUs in the same cluster [40, 41]. Clusters associated with the MC are designated as MC clusters (MCCs). To mitigate intercluster interference, an orthogonal subcarrier is employed to serve all admitted PUs within an MCC. Figure 1b portrays the communication network model integrating the PUC-based downlink H-MA approach for a HetNet configuration, encompassing both MC and SC with accurate CSI. The inclusion of SC further accommodates additional PUs within the MC's coverage area. In addition to MCCs, clusters associated with SC are termed SC clusters (SCCs). Figure 1c illustrates the communication network model incorporating the PUC-based downlink H-MA method within a UAV-assisted HetNet setting, involving MC, SC, and UAV with precise CSI. By incorporating energy-efficient UAV, a larger number of PUs can be accommodated within the MC's coverage. In addition to MCCs and SCCs, clusters tied to UAVs are designated as UAV clusters (UAVCs). Across all network models, subcarriers are allocated based on the subsequent criteria: OMA is employed when a subcarrier is allocated to a cluster with only one PU, whereas NOMA is used when a subcarrier is allocated to a cluster with multiple PUs.

Let $\mathcal{N} = \{1, 2, ..., N\}$ represent the set of all PUs across each of the networks depicted in Fig. 1. The collection of MCCs is denoted as $\mathcal{M} = \{M_1, M_2, ..., M_C\}$, while the assembly of SCCs is labeled as $\mathcal{S} = \{S_1, S_2, ..., S_C\}$. Similarly, the array of UAVCs is symbolized as $\mathcal{U} = \{U_1, U_2, ..., U_C\}$. In the context of the MC-only network, the set $\mathcal{B} = \{MC\}$ signifies the cell comprising the MC. For each MCC M_c, $\mathcal{N}^{M_c} = \{1^{M_c}, 2^{M_c}, ..., N^{M_c}\}$ encompasses all the PUs admitted to M_c. Additionally, $\mathcal{N}_b^{M_c} = \{1_b^{M_c}, 2_b^{M_c}, ..., N_b^{M_c}\}$ designates the PUs admitted to MCC M_c associated with MC b. It is ensured that the summation of PUs admitted within all MCCs linked with MC does not surpass the total count of PUs in the network, i.e., $\sum_{M_c \in \mathcal{M}} N_b^{M_c} \leq N$.

Within the HetNet context, the set of base stations or cells encompasses both a MC and a SC, denoted as $\mathcal{B} = \{MC, SC\}$. In addition to N^{M_c}, $\mathcal{N}^{S_c} = \{1^{S_c}, 2^{S_c}, ..., N^{S_c}\}$ signifies the PUs admitted to SCC S_c. Similarly, we utilize the notation $\mathcal{N}_b^{S_c} = \{1_b^{S_c}, 2_b^{S_c}, ..., N_b^{S_c}\}$ to represent the count of PUs admitted within the SCC associated with SC b. The summation of all PUs admitted in MCCs associated with MC and SCCs associated with SC is defined as $\sum_{M_c \in \mathcal{M}} N_b^{M_c} + \sum_{S_c \in \mathcal{S}} N_b^{S_c}$. It is ensured that $\sum_{M_c \in \mathcal{M}} N_b^{M_c} + \sum_{S_c \in \mathcal{S}} N_b^{S_c} \leq N$, which ensures that the aggregate number of PUs admitted within all MCCs linked to MC and all SCCs tied to SC does not surpass the total number of PUs in the network.

Within the context of the UAV-assisted HetNet, the cellular composition comprises a MC, a SC, and an UAV, denoted as $\mathcal{B} = \{MC, SC, UAV\}$. In addition to N^{M_c} and N^{S_c}, $\mathcal{N}^{U_c} = \{1^{U_c}, 2^{U_c}, ..., N^{U_c}\}$ signifies the PUs admitted to UAVC U_c. Correspondingly, we employ the notation $\mathcal{N}_b^{U_c} = \{1_b^{U_c}, 2_b^{U_c}, ..., N_b^{U_c}\}$ to denote the count of PUs admitted within the UAVC linked to UAV b. The summation of all admitted PUs in MCCs associated with MC, SCCs linked to SC, and UAVCs connected to the UAV is expressed as $\sum_{M_c \in \mathcal{M}} N_b^{M_c} + \sum_{S_c \in \mathcal{S}} N_b^{S_c} + \sum_{U_c \in \mathcal{U}} N_b^{U_c}$. This ensures that $\sum_{M_c \in \mathcal{M}} N_b^{M_c} + \sum_{S_c \in \mathcal{S}} N_b^{S_c} + \sum_{U_c \in \mathcal{U}} N_b^{U_c} \leq N$, ensuring that the collective number of admitted PUs in all MCCs related to MC, all SCCs tied to SC, and all UAVCs associated

Table 2 Research gaps

Sr. No.	Research gaps
i	Present investigations have explored a range of dimensions, spanning from networks solely relying on MC to HetNet, MA techniques, PUC, and the integration of UAVs. However, these elements have been individually studied without being collectively assessed
ii	A notable gap is evident in the comprehensive examination of the interplay between HetNet, H-MA, PUC, and UAV, as highlighted by the findings presented in Table 1
iii	Furthermore, to the best of our knowledge, there has been a lack of research that simultaneously considers various facets, encompassing PU admission within clusters, PU-cell affiliation, PU power distribution, PU fair association with cell (PUFAC), and the optimization of throughput and EE, all integrated within the framework of PUC-based downlink H-MA within UAV-assisted HetNet

Table 3 Contributions

Sr. No.	Contributions
i	This research presents a novel mathematical model and network framework designed to enhance the efficiency of the network by employing the PUC-based downlink H-MA approach. This methodology is specifically tailored for application within UAV-assisted HetNet to optimize both throughput and EE
ii	The problem is formulated as concave fractional programming (CFP) problem and Charnes-Cooper transformation (CCT) is employed to convert it into concave optimization problem, i.e., MINLP. The MINLP problem is acknowledged for its status as a non-deterministic polynomial-time hard (NP-hard)
iii	To achieve an approximation of optimal solutions while reducing complexity, an OAA incorporating ϵ-optimality is employed to tackle the MINLP issue
iv	The efficacy of the PUC-based downlink H-MA approach within UAV-assisted HetNet is evaluated
v	PIs encompassing the optimization of throughput and EE, the inclusion of PUs within clusters, PU-cell affiliations, adherence to minimum QoS rate standards, and the equitable allocation of PUs to cells (PUFAC) are considered in this context
vi	The Jain fairness index (JFI) is utilized to secure equitable allocation of PUs across MC and SC within the HetNet and among MC, SC, and UAV within the UAV-assisted HetNets, thereby ensuring fairness in the process of cell-association
vii	A complexity assessment is conducted using F-Flops and the Big O notation, comparing the proposed ϵ-optimal OAA with an exhaustive search algorithm (ESA) to analyze their computational complexities
viii	The method presented, denoted as PUC-based downlink H-MA, is thoroughly examined to assess its efficacy in various scenarios, including networks composed solely of MC, HetNet, and cases involving the integration of UAV within HetNet
ix	The proposed strategy, i.e., PUC-based downlink H-MA in UAV assisted HetNet, is compared with the most related work done in [21] to assess its performance efficiency and validation of the theoretical work

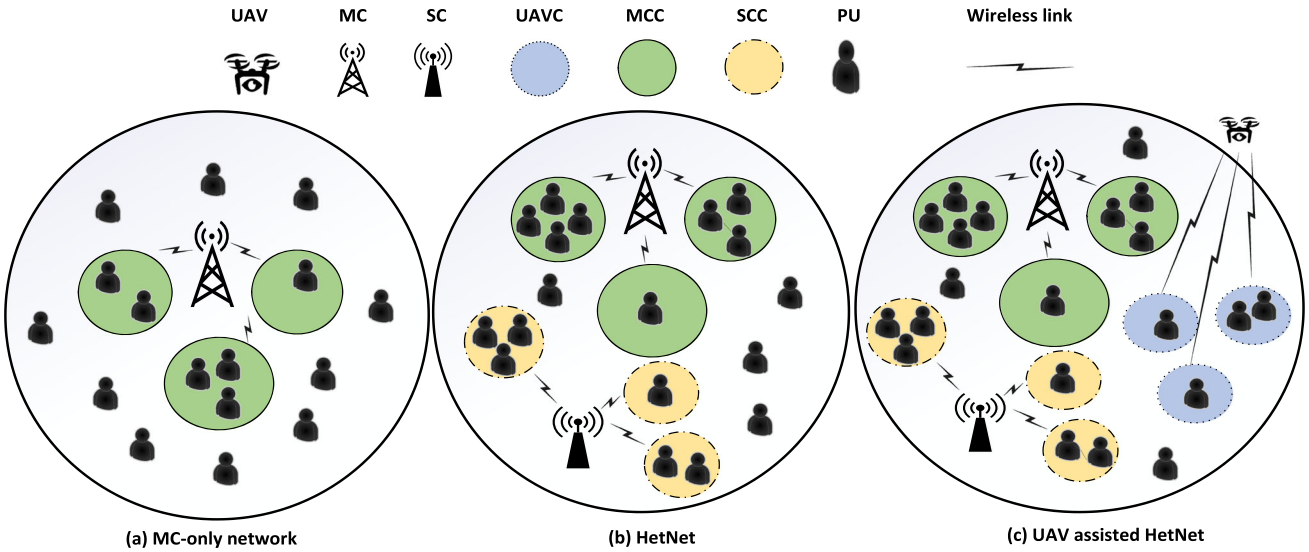

Fig. 1 PUC based downlink H-MA

with the UAV does not exceed the total number of PUs in the network.

Let $g^{n_b^{M_c}} = \tilde{g}^{n_b^{M_c}} \xi G_o \left(\frac{d_o}{d^{n_b^{M_c}}}\right)^{\alpha}$ symbolize the channel coefficient between PU n admitted in MCC M_c and MC b. In this context, $\tilde{g}^{n_b^{M_c}}$ denotes a Rayleigh random variable, ξ represents Gaussian zero-mean shadowing, G_o stands for antenna gain, α signifies the path loss exponent, d_o is the far-field reference distance, and $d^{n_b^{M_c}}$ stands for the distance between admitted PU n in MCC M_c and MC b. Similarly, $g^{n_b^{S_c}} = \tilde{g}^{n_b^{S_c}} \xi G_o \left(\frac{d_o}{d^{n_b^{S_c}}}\right)^{\alpha}$ signifies the channel coefficient between PU n admitted in SCC S_c and SC b, where $d^{n_b^{S_c}}$ represents the distance between admitted PU n in SCC S_c and SC b. Likewise, $g^{n_b^{U_c}} = \tilde{g}^{n_b^{U_c}} \xi G_o \left(\frac{d_o}{d^{n_b^{U_c}}}\right)^{\alpha}$ corresponds to the channel coefficient between PU n admitted in UAVC U_c and UAV b, with $d^{n_b^{U_c}}$ denoting the distance between admitted PU n in UAVC U_c and UAV b. The remaining definitions for these terms remain consistent with those of $g^{n_b^{M_c}}$ [42, 43].

2.1 PUC based downlink H-MA for MC-only network

NOMA implements power domain transmission at the cell to convey information, while the receiving end PUs employ successive interference cancellation (SIC) to extract information by eliminating interference from other PUs. The binary indicator $x^{n^{M_c}}$, depicted in Eq. (1), is assumed to indicate whether PU n is admitted in M_c.

$$x^{n^{M_c}} = \begin{cases} 1, & \text{if } n \text{ is admitted in } M_c \\ 0, & \text{otherwise} \end{cases} \tag{1}$$

The binary indicator $y^{n_b^{M_c}}$, as elucidated in eq. (2), is considered to signify whether PU n that has been previously admitted to M_c is linked with MC b.

$$y^{n_b^{M_c}} = \begin{cases} 1, & \text{if } n \text{ admitted in } M_c \text{ is associated with } b \\ 0, & \text{otherwise} \end{cases} \tag{2}$$

Within a cluster, PUs have the capability to employ SIC for information decoding, subject to the following condition:

- PU n has the option to employ SIC if the signal-to-interference-plus-noise ratio (SINR) received by PU n for the signal from PU i is greater than or equal to the SINR received by PU i.

For the successful decoding and removal of PU i's signal from the signal of PU n admitted in MCC M_c, it is essential for the subsequent inequality to be satisfied, as illustrated in eq. (3).

$$\begin{aligned} &\Omega^{n_b^{M_c}}(i) \geq \Omega^{i_b^{M_c}}(i), \ \ \forall\ i, n \in \mathcal{N} \\ &g^{i_b^{M_c}} \leq g^{n_b^{M_c}}, \ \ \forall\ i \neq n \end{aligned} \tag{3}$$

The PUs within MCC M_c are arranged in an ascending sequence according to their channel gains, as specified in Eq. (4).

$$g^{1_b^{M_c}} \leq g^{2_b^{M_c}} \ldots \leq \ldots g^{N_b^{M_c}} \tag{4}$$

The PUs admitted into MCC M_c receive power in the order stipulated by Eq. (5).

$$p^{1_b^{M_c}} \geq p^{2_b^{M_c}} \ldots \geq \ldots p^{N_b^{M_c}} \tag{5}$$

In order to apportion the overall power of the MC, denoted as $\mathcal{P}^{MC}$, across all the MCCs, it is postulated that the summation $\sum_{M_c=1}^{M_C} p_b^{M_c}$ remains within the bounds of $\mathcal{P}^{MC}$. To establish fairness in power allocation while considering diverse channel gains, a weighting factor $1 \geq l^{n_b^{M_c}} > 0$ is introduced. This coefficient assigns less power to PUs with greater channel gains and conversely, as expressed in Eq. (6) [44].

$$l^{n_b^{M_c}} = 1 - \frac{x^{n^{M_c}} y^{n_b^{M_c}} g^{n_b^{M_c}}}{\sum_{i^{M_c}=n^{M_c}+1}^{N^{M_c}} l^{n_b^{M_c}}} \tag{6}$$

A value of $l^{n_b^{M_c}}$ equating to 1 signifies the absence of any admitted PUs in MCC M_c linked with MC b. The received power for each PU, labeled as $p^{n_b^{M_c}}$, is derived by the multiplication of $l^{n_b^{M_c}}$ and p^{M_c}, representing the designated power allocation for MCC M_c associated with MC b.

2.2 PUC based downlink H-MA for HetNet

For simplification purposes, a single SC has been introduced alongside the MC in the HetNet to improve PU admission, association, as well as throughput and EE enhancement [45]. Furthermore, we incorporate an additional binary indicator, denoted as $x^{n^{S_c}}$, in addition to $x^{n^{M_c}}$, which signifies the admission of PU n into SCC S_c, as outlined in eq. (7).

$$x^{n^{S_c}} = \begin{cases} 1, & \text{if } n \text{is admitted in} S_c \\ 0, & \text{otherwise} \end{cases} \tag{7}$$

Furthermore, as a complement to the already established indicators $y^{n_b^{M_c}}$, we introduce an additional binary indicator denoted as $y^{n_b^{S_c}}$. This indicator signifies whether PU n has been admitted into S_c that is associated with SC s, as illustrated in Eq. (8).

$$y^{n_b^{S_c}} = \begin{cases} 1, & \text{if } n \text{admitted in} S_c \text{ is associated with } b \\ 0, & \text{otherwise} \end{cases} \tag{8}$$

The JFI, as previously introduced in literature [46–48], is utilized in this paper to ensure equitable PU association with both MC and SC within the HetNet. The incorporation of this fairness index serves as a pivotal mechanism for maintaining a well-balanced distribution of traffic loads among all cells present in the network. The JFI is expressed by the following formula:

$$\Psi^{n_b} = \frac{\left(\sum_{n\in\mathcal{N}} (y^{n_b^{M_c}} + y^{n_b^{S_c}})\right)^2}{N \sum_{n\in\mathcal{N}} (y^{n_b^{M_c}})^2 + (y^{n_b^{S_c}})^2}, \ \forall\ b \in \mathcal{B} \tag{9}$$

Here, the variable Ψ^{n_b} is constrained within the range of 0 to 1. Similarly, the arrangement of PUs within S_c is determined by sorting them in ascending order based on their channel gains, as defined in Eq. (10).

$$g^{1_b^{S_c}} \leq g^{2_b^{S_c}} \ldots \leq \ldots g^{N_b^{S_c}} \tag{10}$$

Consequently, the sequence of power allocation for the PUs admitted in S_c is defined by the Eq. (11).

$$p^{1_b^{S_c}} \geq p^{2_b^{S_c}} \ldots \geq \ldots p^{N_b^{S_c}} \tag{11}$$

The distribution of power among the SCCs adheres to the constraint $\sum_{S_c=1}^{S_C} p_b^{S_c} \leq \mathcal{P}^{SC}$, where $\mathcal{P}^{SC}$ signifies the total power of SC. To ensure power allocation based on channel gain, a weighting factor $l^{n_b^{S_c}}$ is introduced, satisfying the condition $1 \geq l^{n_b^{S_c}} > 0$. This factor guarantees that PUs with higher channel gains receive proportionally less power allocation and vice versa, as expressed in Eq. (12).

$$l^{n_b^{S_c}} = 1 - \frac{x^{n^{S_c}} y^{n_b^{S_c}} g^{n_b^{S_c}}}{\sum_{i^{S_c}=n^{S_c}+1}^{N^{S_c}} g^{n_b^{S_c}}} \tag{12}$$

The power allocation for the PUs admitted in the SCC associated with SC is determined by the value of $l^{n_b^{S_c}}$, where $l^{n_b^{S_c}} = 1$ indicates the absence of any admitted PU in that particular SCC. The received power for the PUs admitted in the SCC is calculated as $p^{n_b^{S_c}} = l^{n_b^{S_c}} * p_b^{S_c}$. These weighting factors, namely $l^{n_b^{M_c}}$ and $l^{n_b^{S_c}}$, play a pivotal role in ensuring fairness in the allocation of power among PUs based on their respective channel gains. Their implementation is instrumental in achieving a well-balanced power distribution across the network.

NOMA's power domain multiplexing enables simultaneous resource sharing among PUs, leading to increased throughput and EE. OMA provides resource allocation, optimizing utilization based on channel conditions. This OMA, combined with NOMA, facilitates efficient capacity offloading from MC to SC, reducing congestion and enhancing overall network efficiency. Additionally, NOMA's inherent interference management and power control contribute to energy savings, while the combination of NOMA-OMA, i.e.,

H-MA, ensures flexibility and adaptability in response to changing network dynamics. Together, these integrated techniques create a more resilient and efficient communication environment in HetNet.

2.3 PUC based downlink H-MA for UAV assisted HetNet

To enrich the capabilities of the UAV-assisted HetNet in terms of admission, association, throughput, and EE, we have introduced UAVs alongside MCs and SCs. Moreover, to account for the presence of UAVCs, a binary indicator $x^{n^{U_c}}$ has been introduced in addition to $x^{n^{M_c}}$ and $x^{n^{S_c}}$ indicators. This new indicator signifies the admission status of PU n in the UAVC U_c, as elaborated in Eq. (13).

$$x^{n^{U_c}} = \begin{cases} 1, & \text{if } n\text{is admitted in} U_c \\ 0, & \text{otherwise} \end{cases} \tag{13}$$

Furthermore, as a complement to the pre-existing indicators $y^{n_b^{M_c}}$ and $y^{n_b^{S_c}}$, we introduce an additional binary indicator denoted as $y^{n_b^{U_c}}$. This indicator conveys the information about the admission status of PU n in the UAVC U_c associated with the entity labeled as b, as detailed in Eq. (14).

$$y^{n_b^{U_c}} = \begin{cases} 1, & \text{if } n\text{admitted in} U_c \text{ is associated with } b \\ 0, & \text{otherwise} \end{cases} \tag{14}$$

The JFI, as previously introduced in relevant research works [46–48], is applied to ensure equitable association of PU n with MC, SC, and UAV within the UAV-assisted HetNet framework. This fairness index assumes a vital role in promoting an even distribution of traffic load among all the cells within the network. The formula for the JFI is as presented below:

$$\Psi^{n_b} = \frac{\left(\sum_{n\in\mathcal{N}} (y^{n_b^{M_c}} + y^{n_b^{S_c}} + y^{n_b^{U_c}})\right)^2}{N\sum_{n\in\mathcal{N}} (y^{n_b^{M_c}})^2 + (y^{n_b^{S_c}})^2 + (y^{n_b^{U_c}})^2}, \quad \forall\ b \in \mathcal{B} \tag{15}$$

The inequality $1 \geq \Psi^{n_b} \geq 0$ holds in the formula. Similarly, the arrangement of PUs in U_c based on their channel gains is depicted using ascending order in Eq. (16).

$$g^{1_b^{U_c}} \leq g^{2_b^{U_c}} \ldots \leq \ldots g^{N_b^{U_c}} \tag{16}$$

Consequently, the received power among the admitted PUs in U_c adheres to the sequence specified in Eq. (17).

$$p^{1_b^{U_c}} \geq p^{2_b^{U_c}} \ldots \geq \ldots p^{N_b^{U_c}} \tag{17}$$

The power allocation among the UAVCs is governed by the constraint $\sum_{U_c=1}^{U_C} p_b^{U_c} \leq \mathcal{P}^{UAV}$, where $\mathcal{P}^{UAV}$ stands for the total power available to UAVs. To assign power to the PUs while considering their channel gains, a weighting factor denoted as $l^{n_b^{U_c}}$ is introduced. This factor ensures that PUs with higher channel gains receive relatively lower power and vice versa. This relationship is expressed in Eq. (18).

$$l^{n_b^{U_c}} = 1 - \frac{x^{n^{U_c}} y^{n_b^{U_c}} g^{n_b^{U_c}}}{\sum_{i^{U_c}=n^{U_c}+1}^{N^{U_c}} g^{n_b^{U_c}}} \tag{18}$$

The power assigned to the PUs admitted in the UAVC associated with the UAV is influenced by the value of $l^{n_b^{U_c}}$, wherein $l^{n_b^{U_c}} = 1$ signifies the absence of any admitted PU in that specific UAVC. The power received by the admitted PUs in the UAVC is computed as $p^{n_b^{U_c}} = l^{n_b^{U_c}} * p_b^{U_c}$. These weighting factors ($l^{n_b^{M_c}}$, $l^{n_b^{S_c}}$, and $l^{n_b^{U_c}}$) are vital in ensuring an equitable distribution of power among the PUs based on their respective channel gains, thereby contributing to a well-balanced power allocation throughout the network.

Several key parameters such as precise knowledge of CSI, channel gain values, transmission power, subcarrier allocation, and inter-cluster interference influence the effectiveness of UAV assisted downlink communication and their dynamic adjustment based on PUC is crucial. The precise knowledge of CSI is pivotal, enabling accurate communication resource allocation. The clustering strategy, needs careful consideration to optimize coverage and manage interference based on channel gain values. The transmission power and subcarrier allocation based on PUC ensures efficient use of spectral resources. According to the mentioned scenario, PUs are clustered in MCC, or SCC, or UAVC based on channel gain values. Inter-cluster interference is mitigated using orthogonal subcarriers. Subcarriers are allocated based on OMA for single PU cluster and NOMA for multi-PU clusters. Thus, the mentioned approach adjusts these parameters dynamically in real-time, informed by the evolving network conditions and PU distribution, is essential for maximizing the effectiveness of UAV-assisted downlink communication.

2.4 SINR model for MC-only network

The PUs situated within the MCC linked to MC encounter interference stemming from other PUs coexisting within the same MCC. The SINR [45] experienced by a PU admitted in MCC M_c and associated with MC b can be expressed using Eq. (19). This eq. effectively captures the SINR, which serves as a metric for assessing the received signal quality, accounting for both the influence of interference originating from other PUs and the inherent noise inherent within the

system.

$$\Omega^{n_b^{M_c}} = \frac{x^{n^{M_c}} y^{n_b^{M_c}} p^{n_b^{M_c}} g^{n_b^{M_c}}}{g^{n_b^{M_c}} \sum_{i^{M_c}=n^{M_c}+1}^{N^{M_c}} p^{i_b^{M_c}} + N_o} \tag{19}$$

The SINR corresponding to a PU admitted within MCC M_c and associated with MC b is influenced by various factors, including the received power of the PU ($p^{n_b^{M_c}}$), the received power of other PUs also admitted in the same MCC and associated with MC b ($p^{i_b^{M_c}}$), the total count of admitted PUs in M_c (N^{M_c}), and the noise power spectral density (N_o). These parameters collectively contribute to the calculation of the SINR, a pivotal metric that gauges the quality of the received signal amidst the presence of both interference and background noise.

In each MCC, the last PU to be admitted is strategically placed to experience the highest channel gain, enabling it to effectively cancel out the signals of all other PUs within the same MCC. In scenarios where a particular MCC hosts only a single PU, interference is absent, thus leading to a power allocation coefficient of 1. For MCCs containing more than one PU, the signal-to-noise ratio (SNR) applicable to a single PU is symbolized as $\Omega^{1_b^{M_c}}$. The presence of multiple PUs within a given MCC permits the utilization of SIC, enabling PUs to decode and remove interfering signals, thereby improving overall information reception quality.

2.5 SINR model for HetNet

Within the HetNet context, PUs encounter supplementary interference originating from SCs, in addition to the interference considerations outlined in the MC-only network scenario. More precisely, when a PU n secures admission in MCC M_c connected to MC b, it confronts interference stemming from SCs. This PU's SINR [49, 50] can be quantified mathematically using the formula provided by Eq. (20).

$$\Omega^{n_b^{M_c}} = \frac{x^{n^{M_c}} y^{n_b^{M_c}} p^{n_b^{M_c}} g^{n_b^{M_c}}}{g^{n_b^{M_c}} \sum_{i^{M_c}=n^{M_c}+1}^{N^{M_c}} p^{i_b^{M_c}} + g^{n_b^{S_c}} \mathcal{P}^{SC} + N_o} \tag{20}$$

The SINR pertaining to the PU n that has been granted admission in SCC S_c linked to SC b, while accounting for the interference stemming from MC, is elucidated through the expression provided by Eq. (21).

$$\Omega^{n_b^{S_c}} = \frac{x^{n^{S_c}} y^{n_b^{S_c}} p^{n_b^{S_c}} g^{n_b^{S_c}}}{g^{n_b^{S_c}} \sum_{i^{S_c}=n^{S_c}+1}^{N^{S_c}} p^{i_b^{S_c}} + g^{n_b^{M_c}} \mathcal{P}^{MC} + N_o} \tag{21}$$

2.6 SINR model for UAV-assisted HetNet

Within the context of UAV-assisted HetNet, PUs encounter supplementary interference originating from UAV, alongside the interference elucidated in the MC-only network and HetNet scenarios. Concretely, when a PU n attains admission within MCC M_c linked to MC b, it contends with interference emanating from SC and UAV. The mathematical expression encapsulating the SINR for this PU is formulated by Eq. (22).

$$\Omega^{n_b^{M_c}} = \frac{x^{n^{M_c}} y^{n_b^{M_c}} p^{n_b^{M_c}} g^{n_b^{M_c}}}{g^{n_b^{M_c}} \sum_{i^{M_c}=n^{M_c}+1}^{N^{M_c}} p^{i_b^{M_c}} + g^{n_b^{S_c}} \mathcal{P}^{SC} + g^{n_b^{U_c}} \mathcal{P}^{UAV} + N_o} \tag{22}$$

The SINR of the PU indexed as n and accepted within SCC S_c linked with SC b, considers the impact of both MC and UAV signal disruptions. This SINR is denoted by Eq. (23) and has been discussed in references.

$$\Omega^{n_b^{S_c}} = \frac{x^{n^{S_c}} y^{n_b^{S_c}} p^{n_b^{S_c}} g^{n_b^{S_c}}}{g^{n_b^{S_c}} \sum_{i^{S_c}=n^{S_c}+1}^{N^{S_c}} p^{i_b^{S_c}} + g^{n_b^{M_c}} \mathcal{P}^{MC} + g^{n_b^{U_c}} \mathcal{P}^{UAV} + N_o} \tag{23}$$

The SINR of the PU identified as n and accepted within UAVC U_c linked with UAV b, accounting for the disruption caused by MC and SC, is formulated using Eq. (24) and has been referenced in works.

$$\Omega^{n_b^{U_c}} = \frac{x^{n^{U_c}} y^{n_b^{U_c}} p^{n_b^{U_c}} g^{n_b^{U_c}}}{g^{n_b^{U_c}} \sum_{i^{U_c}=n^{U_c}+1}^{N^{U_c}} p^{i_b^{U_c}} + g^{n_b^{M_c}} \mathcal{P}^{MC} + g^{n_b^{S_c}} \mathcal{P}^{SC} + N_o} \tag{24}$$

2.7 Achievable throughput model

The attainable throughput for the PU labeled as n within the context of MCC M_c linked with MC b is formulated as indicated in Eq. (25).

$$r^{n_b^{M_c}} = \log_2(1 + \Omega^{n_b^{M_c}}) \tag{25}$$

The throughput attainable by the PU indexed as n within the context of the SCC S_c linked with SC b is denoted by eq. (26).

$$r^{n_b^{S_c}} = \log_2(1 + \Omega^{n_b^{S_c}}) \tag{26}$$

The achievable throughput for the PU n within the context of the UAVC U_c linked with UAV b is formulated as indicated in eq. (27).

$$r^{n_b^{U_c}} = \log_2(1 + \Omega^{n_b^{U_c}}) \tag{27}$$

2.8 Problem formulation

Within this section, we establish original optimization challenges that encompass the inclusion of PU admission into a cluster, the association of PUs with cells, power distribution, equitable PU-to-cell associations (PUFAC), and QoS, all while accounting for downlink H-MA strategies, namely OMA and NOMA schemes. This encompasses scenarios within MC-only network, HetNet, and environments facilitated by UAV in conjunction with HetNet. The objective function and associated limitations for formulating these optimization inquiries across the three diverse settings are delineated herein:

2.8.1 For PUC based downlink H-MA enabled MC-only network

The maximization of PU admissions, PU-cell affiliations, throughput, and EE is realized by employing resource distribution outcomes grounded in the subsequent limitations, which are then integrated into the central goal function. By amalgamating the specified goal function and associated limitations, the optimization challenge centered on downlink H-MA, specifically OMA and NOMA strategies for resource allocation within a MC-only network can be structured as follows:

$$\max_{x,y,p} \frac{\sum_{n=1}^{N}\sum_{b=1}^{B}\sum_{M_c=1}^{M_C} x^{n^{M_c}} y^{n_b^{M_c}} r^{n_b^{M_c}}}{P_{ct} + \sum_{n=1}^{N}\sum_{b=1}^{B}\sum_{M_c=1}^{M_C} p^{n_b^{M_c}}}$$

subject to

$$\begin{aligned}
&C1: \sum_{M_c=1}^{M_C} x^{n^{M_c}} \le 1, \ \ \forall\ n \in \mathcal{N} \\
&C2: y^{n_b^{M_c}} \le 1, \ \ \forall\ n \in \mathcal{N} \\
&C3: y^{n_b^{M_c}} \le x^{n^{M_c}} \\
&C4: \sum_{M_c=1}^{M_C} p_b^{M_c} \le \mathcal{P}^{MC}, \ \ \forall\ MC \in \mathcal{B}, \ \ M_c \in \mathcal{M} \\
&C5: \sum_{n\in\mathcal{N}} p^{n_b^{M_c}} \le l^{n_b^{M_c}} * p_b^{M_c} \\
&C6: r^{n_b^{M_c}} \ge x^{n^{M_c}} y^{n_b^{M_c}} R_{min}^{n} \\
&C7: x^{n^{M_c}} \in \{0,1\} \\
&C8: y^{n_b^{M_c}} \in \{0,1\} \\
&C9: p_b^{M_c} \ge 0 \\
&C10: p^{n_b^{M_c}} \ge 0
\end{aligned} \tag{28}$$

The objective underlying the Eq. (28) aims to maximize PU admissions, PU-cell affiliations, throughput measured in megabits per second (Mbps), and EE measured in Mbps per watt (Mbps/watt), all while adhering to the constraints denoted as $C1$ through $C10$. Constraint $C1$ ensures the exclusive admission of a PU into a MCC M_c at any given instance. Constraint $C2$ enforces the restriction that a PU can only associate with a MC b. Ensuring the continuity of PU affiliations within an MCC is the role of constraint $C3$, while $C4$ is responsible for regulating power distribution across the different MCCs M_c. Allocation of power to individual PUs n within MC b is covered by constraint $C5$. Finally, constraint $C6$ embodies the QoS aspect, stipulating the minimum data rate prerequisites for PU n to be accepted into clusters linked with their respective cells.

2.8.2 Alternative problem formulation

The challenge presented in Eq. (28) involves a concave function in the numerator and a convex function in the denominator, classifying it as a concave fractional programming (CFP) issue, where the real-valued functions defined in R^n are denoted as $r^{n_b^{M_c}}$ and $p^{n_b^{M_c}}$. To address this, we employ a Charnes-Cooper transformation (CCT) technique, which converts the CFP problem in (28) into a concave optimization problem by introducing substitutions $r^{n_b^{M_c}} = \left(\frac{w^{n_b^{M_c}}}{z}\right)$ and $p_b^{M_c} = \left(\frac{w_b^{M_c}}{z}\right)$. The resultant transformed concave optimization problem is presented below:

$$\max_{x,y,z} z \sum_{n=1}^{N}\sum_{b=1}^{B}\sum_{M_c=1}^{M_C} x^{n^{M_c}} y^{n_b^{M_c}} \log_2\left(1 + \frac{x^{n^{M_c}} y^{n_b^{M_c}} w^{n_b^{M_c}} g^{n_b^{M_c}}}{g^{n_b^{M_c}} \sum_{i^{M_c}=n^{M_c}+1}^{N^{M_c}} w^{i_b^{M_c}} + zN_o}\right)$$

subject to

$$\begin{aligned}
&C1: \sum_{M_c=1}^{M_C} x^{n^{M_c}} \le 1, \ \ \forall\ n \in \mathcal{N} \\
&C2: \sum_{b\in\mathcal{B}}\sum_{M_c=1}^{M_C} y^{n_b^{M_c}} \le 1, \ \ \forall\ n \in \mathcal{N} \\
&C3: y^{n_b^{M_c}} \le x^{n^{M_c}} \\
&C4: \sum_{M_c=1}^{M_C} w_b^{M_c} \le \mathcal{P}^{MC} z, \ \ \forall\ MC \in \mathcal{B}, \ \ M_c \in \mathcal{M} \\
&C5: \sum_{n\in\mathcal{N}} w^{n_b^{M_c}} \le l^{n_b^{M_c}} * w_b^{M_c} \\
&C6: \log_2\left(1 + \frac{x^{n^{M_c}} y^{n_b^{M_c}} w^{n_b^{M_c}} g^{n_b^{M_c}}}{g^{n_b^{M_c}} \sum_{i^{M_c}=n^{M_c}+1}^{N^{M_c}} w^{i_b^{M_c}} + zN_o}\right) \\
&\qquad \ge x^{n^{M_c}} y^{n_b^{M_c}} R_{min}^{n} \\
&C7: x^{n^{M_c}} \in \{0,1\}
\end{aligned}$$

$$
\begin{aligned}
&C8: y^{n_b^{M_c}} \in \{0,1\}\\
&C9: w_b^{M_c} \geq 0\\
&C10: w^{n_b^{M_c}} \geq 0\\
&C11: P_{ct} z + \sum_{n\in N}\sum_{b\in B}\sum_{M_c\in\mathcal{M}} w^{n_b^{M_c}} = 1
\end{aligned} \tag{29}
$$

2.8.3 For PUC based downlink H-MA enabled HetNet

The maximization of PU admissions, PU-cell affiliations, throughput, and EE is realized by utilizing resource allocation outcomes guided by the subsequent specified limitations, which are then integrated into the core objective function. Integrating the mentioned objective function and outlined constraints, the optimization challenge rooted in downlink H-MA, encompassing OMA and NOMA strategies for resource allocation within a HetNet can be formulated as follows:

$$
\max_{x,y,p} \frac{\sum_{n=1}^{N}\sum_{b=1}^{B}\left(\sum_{M_c=1}^{M_C} x^{n^{M_c}} y^{n_b^{M_c}} r^{n_b^{M_c}} + \sum_{S_c=1}^{S_C} x^{n^{S_c}} y^{n_b^{S_c}} r^{n_b^{S_c}}\right)}{P_{ct} + \sum_{n=1}^{N}\sum_{b=1}^{B}\left(\sum_{M_c=1}^{M_C} p^{n_b^{M_c}} + \sum_{S_c=1}^{S_C} p^{n_b^{S_c}}\right)}
$$

subject to

$$
\begin{aligned}
&C1: \sum_{M_c=1}^{M_C} x^{n^{M_c}} + \sum_{S_c=1}^{S_C} x^{n^{S_c}} \leq 1, \ \forall\ n \in \mathcal{N}\\
&C2: \sum_{b\in\mathcal{B}}\left(\sum_{M_c=1}^{M_C} y^{n_b^{M_c}} + \sum_{S_c=1}^{S_C} y^{n_b^{S_c}}\right) \leq 1, \ \forall\ n \in \mathcal{N}\\
&C3: y^{n_b^{M_c}} + y^{n_b^{S_c}} \leq x^{n^{M_c}} + x^{n^{S_c}}\\
&C4: \left(\sum_{n\in\mathcal{N}}\left(y^{n_b^{M_c}} + y^{n_b^{S_c}}\right)\right)^2 - N\sum_{n\in\mathcal{N}}\left(y^{n_b^{M_c}} + y^{n_b^{S_c}}\right)^2 \leq 0\\
&C5: \sum_{M_c=1}^{M_C} p_b^{M_c} \leq \mathcal{P}^{MC}, \ \forall\ MC \in \mathcal{B}, \ M_c \in \mathcal{M}\\
&C6: \sum_{S_c=1}^{S_C} p_b^{S_c} \leq \mathcal{P}^{SC}, \quad forall\ SC \in \mathcal{B}, \ S_c \in \mathcal{S}\\
&C7: \sum_{n\in\mathcal{N}} p^{n_b^{M_c}} \leq l^{n_b^{M_c}} * p_b^{M_c}\\
&C8: \sum_{n\in\mathcal{N}} p^{n_b^{S_c}} \leq l^{n_b^{S_c}} * p_b^{S_c}\\
&C9: r^{n_b^{M_c}} \geq x^{n^{M_c}} y^{n_b^{M_c}} R^n_{min}\\
&C10: r^{n_b^{S_c}} \geq x^{n^{S_c}} y^{n_b^{S_c}} R^n_{min}\\
&C11: x^{n^{M_c}} \in \{0,1\}, x^{n^{S_c}} \in \{0,1\}\\
&C12: y^{n_b^{M_c}} \in \{0,1\}, y^{n_b^{S_c}} \in \{0,1\}\\
&C13: p_b^{M_c} \geq 0, p_b^{S_c} \geq 0\\
&C14: p^{n_b^{M_c}} \geq 0, p^{n_b^{S_c}} \geq 0
\end{aligned} \tag{30}
$$

2.8.4 Alternative problem formulation

The challenge presented in Eq. (30) entails a concave function in the numerator and a convex function in the denominator, thereby categorizing it as a CFP problem. Here, the real-valued functions in R^n are denoted as $r^{n_b^{M_c}}$, $p^{n_b^{M_c}}$, as well as $r^{n_b^{S_c}}$ and $p^{n_b^{S_c}}$. To address this, a CCT technique is employed to convert the CFP problem in (30) into a concave optimization problem. This is achieved through the introduction of substitutions $p^{n_b^{M_c}} = \left(\frac{w^{n_b^{M_c}}}{z}\right)$, $p_b^{M_c} = \left(\frac{w_b^{M_c}}{z}\right)$, and $p^{n_b^{S_c}} = \left(\frac{w^{n_b^{S_c}}}{z}\right)$, $p_b^{S_c} = \left(\frac{w_b^{S_c}}{z}\right)$. The equivalent problem is:

$$
\begin{aligned}
&\max_{x,y,z} z\sum_{n=1}^{N}\sum_{b=1}^{B}\Bigg(\sum_{M_c=1}^{M_C} x^{n^{M_c}} y^{n_b^{M_c}}\\
&\log_2\left(1 + \frac{x^{n^{M_c}} y^{n_b^{M_c}} w^{n_b^{M_c}} g^{n_b^{M_c}}}{g^{n_b^{M_c}} \sum_{i^{M_c}=n^{M_c}+1}^{N^{M_c}} w^{i_b^{M_c}} + g^{n_b^{S_c}} \mathcal{P}^{SC} z + zN_o}\right)\\
&+ \sum_{S_c=1}^{S_C} x^{n^{S_c}} y^{n_b^{S_c}}\\
&\log_2\left(1 + \frac{x^{n^{S_c}} y^{n_b^{S_c}} w^{n_b^{S_c}} g^{n_b^{S_c}}}{g^{n_b^{S_c}} \sum_{i^{S_c}=n^{S_c}+1}^{N^{S_c}} w^{i_b^{S_c}} + g^{n_b^{M_c}} \mathcal{P}^{MC} z + zN_o}\right)\Bigg)
\end{aligned}
$$

subject to

$$
\begin{aligned}
&C1: \sum_{M_c=1}^{M_C} x^{n^{M_c}} + \sum_{S_c=1}^{S_C} x^{n^{S_c}} \leq 1, \ \forall\ n \in \mathcal{N}\\
&C2: \sum_{b\in\mathcal{B}}\left(\sum_{M_c=1}^{M_C} y^{n_b^{M_c}} + \sum_{S_c=1}^{S_C} y^{n_b^{S_c}}\right) \leq 1, \ \forall\ n \in \mathcal{N}\\
&C3: y^{n_b^{M_c}} + y^{n_b^{S_c}} \leq x^{n^{M_c}} + x^{n^{S_c}}\\
&C4: \left(\sum_{n\in\mathcal{N}}\left(y^{n_b^{M_c}} + y^{n_b^{S_c}}\right)\right)^2 - N\sum_{n\in\mathcal{N}}\left(y^{n_b^{M_c}} + y^{n_b^{S_c}}\right)^2 \leq 0\\
&C5: \sum_{M_c=1}^{M_C} w_b^{M_c} \leq \mathcal{P}^{MC} z, \ \forall\ MC \in \mathcal{B}, \ M_c \in \mathcal{M}\\
&C6: \sum_{S_c=1}^{S_C} w_b^{S_c} \leq \mathcal{P}^{SC} z, \ \forall\ SC \in \mathcal{B}, \ S_c \in \mathcal{S}\\
&C7: \sum_{n\in\mathcal{N}} w^{n_b^{M_c}} \leq l^{n_b^{M_c}} * w_b^{M_c}\\
&C8: \sum_{n\in\mathcal{N}} w^{n_b^{S_c}} \leq l^{n_b^{S_c}} * w_b^{S_c}\\
&C9: \log_2\left(1 + \frac{x^{n^{M_c}} y^{n_b^{M_c}} w^{n_b^{M_c}} g^{n_b^{M_c}}}{g^{n_b^{M_c}} \sum_{i^{M_c}=n^{M_c}+1}^{N^{M_c}} w^{i_b^{M_c}} + g^{n_b^{S_c}} \mathcal{P}^{SC} z + zN_o}\right)\\
&\geq x^{n^{M_c}} y^{n_b^{M_c}} R^n_{min}\\
&C10: \log_2\left(1 + \frac{x^{n^{S_c}} y^{n_b^{S_c}} w^{n_b^{S_c}} g^{n_b^{S_c}}}{g^{n_b^{S_c}} \sum_{i^{S_c}=n^{S_c}+1}^{N^{S_c}} w^{i_b^{S_c}} + g^{n_b^{M_c}} \mathcal{P}^{MC} z + zN_o}\right)\\
&\geq x^{n^{S_c}} y^{n_b^{S_c}} R^n_{min}\\
&C11: x^{n^{M_c}} \in \{0,1\}, x^{n^{S_c}} \in \{0,1\}\\
&C12: y^{n_b^{M_c}} \in \{0,1\}, y^{n_b^{S_c}} \in \{0,1\}\\
&C13: w_b^{M_c} \geq 0, w_b^{S_c} \geq 0\\
&C14: w^{n_b^{M_c}} \geq 0, w^{n_b^{S_c}} \geq 0\\
&C15: P_{ct} z + \sum_{n\in N}\sum_{b\in B}\left(\sum_{M_c\in\mathcal{M}} w^{n_b^{M_c}} + \sum_{S_c\in\mathcal{S}} w^{n_b^{S_c}}\right) = 1
\end{aligned} \tag{31}
$$

2.8.5 For PUC based downlink H-MA enabled UAV assisted HetNet

The goal of maximizing PU admissions, PU-cell affiliations, throughput, and EE is accomplished by utilizing the outcomes of resource allocation determined by the stipulated constraints and integrated into the core objective function. By integrating the specified objective function and outlined constraints, the optimization problem rooted in downlink H-MA, encompassing OMA and NOMA strategies for resource allocation within a HetNet, can be formulated as follows:

2.8.6 Alternative problem formulation

The challenge presented in Eq. (32) categorizes as a CFP problem. In this context, the real-valued functions existing in R^n are denoted as $r^{n_b^{M_c}}$, $p^{n_b^{M_c}}$, as well as $r^{n_b^{S_c}}$, $p^{n_b^{S_c}}$, and additionally $r^{n_b^{U_c}}$, $p^{n_b^{U_c}}$. To address this challenge, a CCT approach has been employed, converting the CFP problem outlined in (32) into a concave optimization problem through substitutions such as $p^{n_b^{M_c}} = \left(\frac{w^{n_b^{M_c}}}{z}\right)$, $p_b^{M_c} = \left(\frac{w_b^{M_c}}{z}\right)$,

$$\max_{x,y,p} \frac{\sum_{n=1}^{N}\sum_{b=1}^{B}\left(\sum_{M_c=1}^{M_C} x^{n^{M_c}} y^{n_b^{M_c}} r^{n_b^{M_c}} + \sum_{S_c=1}^{S_C} x^{n^{S_c}} y^{n_b^{S_c}} r^{n_b^{S_c}} + \sum_{U_c=1}^{U_C} x^{n^{U_c}} y^{n_b^{U_c}} r^{n_b^{U_c}}\right)}{P_{ct} + \sum_{n=1}^{N}\sum_{b=1}^{B}\left(\sum_{M_c=1}^{M_C} p^{n_b^{M_c}} + \sum_{S_c=1}^{S_C} p^{n_b^{S_c}} + \sum_{U_c=1}^{U_C} p^{n_b^{U_c}}\right)}$$

subject to

$$
\begin{aligned}
&C1: \sum_{M_c=1}^{M_C} x^{n^{M_c}} + \sum_{S_c=1}^{S_C} x^{n^{S_c}} + \sum_{U_c=1}^{U_C} x^{n^{U_c}} \le 1, \ \ \forall\ n \in \mathcal{N}\\
&C2: \sum_{b\in\mathcal{B}}\left(\sum_{M_c=1}^{M_C} y^{n_b^{M_c}} + \sum_{S_c=1}^{S_C} y^{n_b^{S_c}} + \sum_{U_c=1}^{U_C} y^{n_b^{U_c}}\right) \le 1, \ \ \forall\ n \in \mathcal{N}\\
&C3: y^{n_b^{M_c}} + y^{n_b^{S_c}} + y^{n_b^{U_c}} \le x^{n^{M_c}} + x^{n^{S_c}} + x^{n^{U_c}}\\
&C4: \left(\sum_{n\in\mathcal{N}}\left(y^{n_b^{M_c}} + y^{n_b^{S_c}} + y^{n_b^{U_c}}\right)\right)^2 - N\sum_{n\in\mathcal{N}}\left(y^{n_b^{M_c}} + y^{n_b^{S_c}} + y^{n_b^{U_c}}\right)^2 \le 0\\
&C5: \sum_{M_c=1}^{M_C} p_b^{M_c} \le \mathcal{P}^{MC}, \ \ \forall\ MC \in \mathcal{B}, \ \ M_c \in \mathcal{M}\\
&C6: \sum_{S_c=1}^{S_C} p_b^{S_c} \le \mathcal{P}^{SC}, \ \ \forall\ SC \in \mathcal{B}, \ \ S_c \in \mathcal{S}\\
&C7: \sum_{U_c=1}^{U_C} p_b^{U_c} \le \mathcal{P}^{UC}, \ \ \forall\ UAV \in \mathcal{B}, \ \ U_c \in \mathcal{U}\\
&C8: \sum_{n\in\mathcal{N}} p^{n_b^{M_c}} \le l^{n_b^{M_c}} * p_b^{M_c}\\
&C9: \sum_{n\in\mathcal{N}} p^{n_s^{S_c}} \le l^{n_b^{S_c}} * p_b^{S_c}\\
&C10: \sum_{n\in\mathcal{N}} p^{n_b^{U_c}} \le l^{n_b^{U_c}} * p_b^{U_c}\\
&C11: r^{n_b^{M_c}} \ge x^{n^{M_c}} y^{n_b^{M_c}} R_{min}^n\\
&C12: r^{n_b^{S_c}} \ge x^{n^{S_c}} y^{n_b^{S_c}} R_{min}^n\\
&C13: r^{n_b^{U_c}} \ge x^{n^{U_c}} y^{n_b^{U_c}} R_{min}^n\\
&C14: x^{n^{M_c}} \in \{0,1\}, x^{n^{S_c}} \in \{0,1\}, x^{n^{U_c}} \in \{0,1\}\\
&C15: y^{n_b^{M_c}} \in \{0,1\}, y^{n_b^{S_c}} \in \{0,1\}, y^{n_b^{U_c}} \in \{0,1\}\\
&C16: p_b^{M_c} \ge 0, p_b^{S_c} \ge 0, p_b^{U_c} \ge 0\\
&C17: p^{n_b^{M_c}} \ge 0, p^{n_b^{S_c}} \ge 0, p^{n_b^{U_c}} \ge 0
\end{aligned}
\tag{32}
$$

$p^{n_b^{S_c}} = \left(\frac{w^{n_b^{S_c}}}{z}\right)$, $p_b^{S_c} = \left(\frac{w_b^{S_c}}{z}\right)$, and $p^{n_b^{U_c}} = \left(\frac{w^{n_b^{U_c}}}{z}\right)$, $p_b^{U_c} = \left(\frac{w_b^{U_c}}{z}\right)$. The equivalent concave optimization problem is presented below:

The problems described in Eqs. (29), (31), and (33) exhibit a NP-hard nature and fall into the category of MINLP. The inclusion of discrete variables within polynomial time introduces complexities in finding optimal solutions using any

$$\max_{x,y,z} z \sum_{n=1}^{N}\sum_{b=1}^{B}\Bigg(\sum_{M_c=1}^{M_C} x^{n^{M_c}} y^{n_b^{M_c}} \log_2\left(1+\frac{x^{n^{M_c}} y^{n_b^{M_c}} w^{n_b^{M_c}} g^{n_b^{M_c}}}{g^{n_b^{M_c}} \sum_{i^{M_c}=n^{M_c}+1}^{N^{M_c}} w^{i_b^{M_c}} + g^{n_b^{S_c}} \mathcal{P}^{SC} z + g^{n_b^{U_c}} \mathcal{P}^{UAV} z + zN_o}\right)$$
$$+\sum_{S_c=1}^{S_C} x^{n^{S_c}} y^{n_b^{S_c}} \log_2\left(1+\frac{x^{n^{S_c}} y^{n_b^{S_c}} w^{n_b^{S_c}} g^{n_b^{S_c}}}{g^{n_b^{S_c}} \sum_{i^{S_c}=n^{S_c}+1}^{N^{S_c}} w^{i_b^{S_c}} + g^{n_b^{M_c}} \mathcal{P}^{MC} z + g^{n_b^{U_c}} \mathcal{P}^{UAV} z + zN_o}\right)$$
$$+\sum_{U_c=1}^{U_C} x^{n^{U_c}} y^{n_b^{U_c}} \log_2\left(1+\frac{x^{n^{U_c}} y^{n_b^{U_c}} w^{n_b^{U_c}} g^{n_b^{U_c}}}{g^{n_b^{U_c}} \sum_{i^{U_c}=n^{U_c}+1}^{N^{U_c}} w^{i_b^{U_c}} + g^{n_b^{M_c}} \mathcal{P}^{MC} z + g^{n_b^{S_c}} \mathcal{P}^{SC} z + zN_o}\right)\Bigg)$$

subject to

$$C1: \sum_{M_c=1}^{M_C} x^{n^{M_c}} + \sum_{S_c=1}^{S_C} x^{n^{S_c}} + \sum_{U_c=1}^{U_C} x^{n^{U_c}} \le 1, \forall n \in \mathcal{N}$$

$$C2: \sum_{b\in\mathcal{B}}\left(\sum_{M_c=1}^{M_C} y^{n_b^{M_c}} + \sum_{S_c=1}^{S_C} y^{n_b^{S_c}} + \sum_{U_c=1}^{U_C} y^{n_b^{U_c}}\right) \le 1, \forall n \in \mathcal{N}$$

$$C3: y^{n_b^{M_c}} + y^{n_b^{S_c}} + y^{n_b^{U_c}} \le x^{n^{M_c}} + x^{n^{S_c}} + x^{n^{U_c}}$$

$$C4: \left(\sum_{n\in\mathcal{N}}(y^{n_b^{M_c}} + y^{n_b^{S_c}} + y^{n_b^{U_c}})\right)^2 - N\sum_{n\in\mathcal{N}}(y^{n_b^{M_c}} + y^{n_b^{S_c}} + y^{n_b^{U_c}})^2 \le 0 C5: \sum_{M_c=1}^{M_C} w_b^{M_c} \le \mathcal{P}^{MC} z, \forall MC \in \mathcal{B}, M_c \in \mathcal{M}$$

$$C6: \sum_{S_c=1}^{S_C} w_b^{S_c} \le \mathcal{P}^{SC} z, \forall SC \in \mathcal{B}, S_c \in \mathcal{S}$$

$$C7: \sum_{U_c=1}^{U_C} w_b^{U_c} \le \mathcal{P}^{UAVC} z, \forall UAV \in \mathcal{B}, U_c \in \mathcal{U}$$

$$C8: \sum_{n\in\mathcal{N}} w^{n_b^{M_c}} \le l^{n_b^{M_c}} * w_b^{M_c}$$

$$C9: \sum_{n\in\mathcal{N}} w^{n_b^{S_c}} \le l^{n_b^{S_c}} * w_b^{S_c}$$

$$C10: \sum_{n\in\mathcal{N}} w^{n_b^{U_c}} \le l^{n_b^{U_c}} * w_b^{U_c}$$

$$C11: \log_2\left(1+\frac{x^{n^{M_c}} y^{n_b^{M_c}} w^{n_b^{M_c}} g^{n_b^{M_c}}}{g^{n_b^{M_c}} \sum_{i^{M_c}=n^{M_c}+1}^{N^{M_c}} w^{i_b^{M_c}} + g^{n_b^{S_c}} \mathcal{P}^{SC} z + g^{n_b^{U_c}} \mathcal{P}^{UAV} z + zN_o}\right) \ge x^{n^{M_c}} y^{n_b^{M_c}} R_{min}^n$$

$$C12: \log_2\left(1+\frac{x^{n^{S_c}} y^{n_b^{S_c}} w^{n_b^{S_c}} g^{n_b^{S_c}}}{g^{n_b^{S_c}} \sum_{i^{S_c}=n^{S_c}+1}^{N^{S_c}} w^{i_b^{S_c}} + g^{n_b^{M_c}} \mathcal{P}^{MC} z + g^{n_b^{U_c}} \mathcal{P}^{UAV} z + zN_o}\right) \ge x^{n^{S_c}} y^{n_b^{S_c}} R_{min}^n$$

$$C13: \log_2\left(1+\frac{x^{n^{U_c}} y^{n_b^{U_c}} w^{n_b^{U_c}} g^{n_b^{U_c}}}{g^{n_b^{U_c}} \sum_{i^{U_c}=n^{U_c}+1}^{N^{U_c}} w^{i_b^{U_c}} + g^{n_b^{M_c}} \mathcal{P}^{MC} z + g^{n_b^{S_c}} \mathcal{P}^{SC} z + zN_o}\right) \ge x^{n^{U_c}} y^{n_b^{U_c}} R_{min}^n$$

$$C14: x^{n^{M_c}} \in \{0,1\}, x^{n^{S_c}} \in \{0,1\}, x^{n^{U_c}} \in \{0,1\}$$

$$C15: y^{n_b^{M_c}} \in \{0,1\}, y^{n_b^{S_c}} \in \{0,1\}, y^{n_b^{U_c}} \in \{0,1\}$$

$$C16: w_b^{M_c} \ge 0, w_b^{S_c} \ge 0, w_b^{U_c} \ge 0$$

$$C17: w^{n_b^{M_c}} \ge 0, w^{n_b^{S_c}} \ge 0, w^{n_b^{U_c}} \ge 0$$

$$C18: P_{cl} z + \sum_{n\in N}\sum_{b\in B}\Big(\sum_{M_c\in\mathcal{M}} w^{n_b^{M_c}} + \sum_{S_c\in\mathcal{S}} w^{n_b^{S_c}} + \sum_{U_c\in\mathcal{U}} w^{n_b^{U_c}}\Big) = 1 \tag{33}$$

algorithm. This issue involves both binary variables, such as $x^{n^{M_c}}$, $x^{n^{S_c}}$, $x^{n^{U_c}}$, and $y^{n_b^{M_c}}$, $y^{n_b^{S_c}}$, $y^{n_b^{U_c}}$, as well as continuous variables like $w_b^{M_c}$, $w_b^{S_c}$, $w_b^{U_c}$, and $w^{n_b^{M_c}}$, $w^{n_b^{S_c}}$, $w^{n_b^{U_c}}$. As the number of PUs (N) increases, the search space in problems (29), (31), and (33) grows exponentially, leading to computational challenges. While an ESA could yield an optimal solution through binary variable exploration, its complexity is considerable, as it requires solving $2^{|N|}$ optimization problems for binary variable search space of $2^{|N|}$. Thus, to address this, we propose the OAA to attain a near-optimal solution ensuring convergence [51]. The detailed implementation of OAA [51] for the MINLP problems outlined in eqs. (29), (31), and (33) is presented in the subsequent section. Additional details and the complete transformation process from CFP problem to MINLP problem using CCT can be found in Appendix A. The symbols employed in the model are elaborated in Table 4.

3 Proposed solution

Equations (29), (31), and (33) encompass a mix of integer, binary, and continuous variables, which categorizes them as instances of MINLP problems. The binary variables, encompassing $x^{n^{M_c}}$, $y^{n_b^{M_c}}$, $x^{n^{S_c}}$, $y^{n_b^{S_c}}$, $x^{n^{U_c}}$, and $y^{n_b^{U_c}}$, capture PU admissions and associations within diverse network contexts. The integer variables capture PU counts admitted in MCC, MCC/SCC, or MCC/SCC/UAVC, while continuous variables such as received power, SINR, throughput, and EE quantify pertinent metrics. This section introduces the ϵ-optimal OAA as a resolution for tackling the formulated problems in Eqs. (29), (31), and (33).

In Eqs. (29), (31), and (33), the objective function denoted as $\mathcal{A}$ and the set of constraints β_{C1-Cv} are collectively indicated by $\theta = \tau \cup \psi$, where τ encompasses the binary variables linked with PU admissions in clusters and PU associations with cells, and ψ involves the continuous variables associated with the received power received by the admitted PUs within clusters connected to the cells. Equations (29), (31), and (33) constitute the problem formulations that adhere to the ensuing propositions.

1) The set ψ is bounded, convex, and not devoid of elements. When the values of θ are held constant, both the objective function $\mathcal{A}$ and the constraints β_{C1-Cv} demonstrate convexity with respect to ψ.
2) The objective function $\mathcal{A}$ and the constraints β_{C1-Cv} possess continuous differentiability.
3) Each nonlinear, continuous subproblem can be effectively addressed by maintaining the values of θ in a manner that fulfills the prescribed constraints.
4) Upon stabilizing θ, the nonlinear programming (NLP) dilemma can be precisely resolved.

The issues delineated in Eqs. (29), (31), and (33) align with the MINLP category, in accordance with the outlined propositions. To address these challenges, an OAA methodology, detailed in [52], is applied. OAA leverages linear approximations to tackle the problems defined in Eqs. (29), (31), and (33). By employing OAA, all four propositions pertaining to these problems are fulfilled through the utilization of ascending lower bounds and descending upper bounds. The convergence of the OAA with a predefined tolerance ϵ ensures its finite iterations and ultimate convergence, as highlighted in [53].

To generate sequences of upper and lower bounds, the MINLP challenges presented in Eqs. (29), (31), and (33) are disassembled into primal and master problems. The primal problem arises by establishing the value of the binary variable θ as θ^i during the i-th iteration. Formulated through the OAA methodology [52, 53], the primal problem can be represented as Eq. (34).

$$\begin{aligned} &\min_{\psi} \quad -\mathcal{A}\left(\theta^i, \psi\right) \\ &\text{subject to} \\ &\beta_{C1-Cv}\left(\theta^i, \psi\right) \leq 0 \end{aligned} \tag{34}$$

The problem articulated in Eq. (34) is addressed to ascertain the value of θ^i, which is then employed within the context of the master problem [54]. The solution obtained through the primal problem serves as an upper bound, while the master problem is tackled to establish a lower bound. The adoption of the OAA methodology involves linearizing the objective function $\mathcal{A}$ and the constraint function β_{C1-Cv} centered around the primal solution ψ^i [55, 56]. Solving the master problem yields the integer variable θ^{i+1} for the ensuing iteration. This iterative process continues until the disparity between the upper and lower bound values is equal to or less than a predetermined threshold ϵ. The issues introduced in Eqs. (29), (31), and (33) are transformed as illustrated in Eq. (35) [52, 53]. Algorithm 1, presents the pseudocode for the application of the OAA to resolve the problems delineated in Eqs. (29), (31), and (33).

$$\begin{aligned} &\min_{\theta} \min_{\psi} \quad -\mathcal{A}\left(\theta^i, \psi\right) \\ &\text{subject to} \\ &\beta_{C1-Cv}\left(\theta^i, \psi\right) \leq 0 \end{aligned} \tag{35}$$

Table 4 Symbols

Symbol	Definition
N	Overall count of PUs uniformly distributed in the network
$\mathcal{B}$	Cells or base stations collection, i.e., MC in MC-only network, MC, and SC in and in HetNet, MC, SC, and UAV in UAV assisted HetNet
$\mathcal{M}$	Set of MCCs
$\mathcal{S}$	Set of SCCs
$\mathcal{U}$	Set of UAVCs
M_c	Cluster with MC, i.e., MCC
M_C	Total clusters with MC, i.e., MCCs
S_c	Cluster with SC, i.e., SCC
S_C	Total clusters with SC, i.e., SCCs
U_c	Cluster with UAV, i.e., UAVC
U_C	Total clusters with UAV, i.e., UAVCs
$N^{M_c}, N^{S_c}, N^{U_c}$	Admitted PUs in M_c, S_c, U_c, respectively
$N_b^{M_c}$	PUs admitted in M_c associated to b
$N_b^{S_c}$	PUs that are admitted into S_c and linked to b
$N_b^{U_c}$	PUs that are admitted in U_c and associated with b
$g^{n_b^{M_c}}$	Channel gain between n admitted in M_c and MC b
$\tilde{g}^{n_b^{M_c}}$	PU's channel rayleigh random variable with MC
$g^{n_b^{S_c}}$	Channel gain between the admitted n in S_c and the SC b
$\tilde{g}^{n_b^{S_c}}$	PU's channel rayleigh random variable with SC
$g^{n_b^{U_c}}$	Channel gain between the admitted n in U_c and the UAV b
$\tilde{g}^{n_b^{U_c}}$	PU's channel rayleigh random variable with UAV
α	The numerical value of the path loss exponent
$d^{n_b^{M_c}}$	Admitted PU's distance from the MC b
$x^{n^{M_c}}$	Binary variable denoting the admission status of n in M_c
$d^{n_b^{S_c}}$	Admitted PU's distance from the SC b
$x^{n^{S_c}}$	Binary variable indicating the admission status of n in S_c
$d^{n_b^{U_c}}$	Admitted PU's distance from the UAV b
$x^{n^{U_c}}$	Binary variable representing the admission status of n in U_c
$y^{n_b^{M_c}}$	Binary association variable for association of n with the MC
$\Omega^{n_b^{M_c}}$	SINR of n admitted in M_c associated with b
$\Omega^{n_b^{S_c}}$	SINR of n admitted in S_c associated with b
$\Omega^{n_b^{U_c}}$	SINR of n admitted in U_c associated with b
$y^{n_b^{S_c}}$	Binary association variable for association of n with SC
$y^{n_b^{U_c}}$	Binary association variable for association of n with UAV
$l^{n_b^{M_c}}, l^{n_b^{S_c}}, l^{n_b^{U_c}}$	Weighting factor for power allocation to n admitted in MCC, SCC, UAVC, respectively
$\mathcal{P}^{MC}, \mathcal{P}^{SC}, \mathcal{P}^{UAV}$	The overall power at the MC, SC, UAV, respectively
d_o	Reference distance used for far-field calculations
$p_b^{M_c}$	Power allocated for M_c associated with b
N_o	Power spectral density of the noise
$p_b^{S_c}$	Power allocated for S_c associated with b
G_o	Gain of the antenna

Table 4 continued

Symbol	Definition
$p_b^{U_c}$	Allocated power for U_c associated with b
ξ	Zero-mean Gaussian random variable
$p^{n_b^{M_c}}$	Power received by n in M_c associated with MC
$r^{n_b^{M_c}}$	Throughput achievable for n in M_c associated with MC
$p^{n_b^{S_c}}$	Power received by n in S_c associated with SC
σ	Spread or standard deviation
$r^{n_b^{S_c}}$	Throughput achievable for n in S_c associated with SC
$p^{n_b^{U_c}}$	Power received by n in U_c associated with UAV
$r^{n_b^{U_c}}$	Attainable data rate for n in U_c linked with UAV
R_{min}^n	Minimum throughput needed for the PU n
Ψ^{n_b}	JFI

Algorithm 1: Outer **a**pproximation **a**lgorithm

$i \leftarrow 1$
Initialize θ
$\epsilon \leftarrow 10^{-3}$
$Convergence \leftarrow FALSE$
while $Convergence == FALSE$ **do**
$\psi^i \leftarrow \begin{cases} \arg\min\limits_{\psi} & -\mathcal{A}(\theta, \psi) \\ \text{subject to} & \beta_{C1-Cv}(\theta, \psi) \leq 0; \end{cases}$
Upper Bound $\leftarrow \mathcal{A}\left(\theta^i, \psi^*\right)$
$(\theta^*, \psi^*, \Upsilon^*) \leftarrow \begin{cases} \arg\min\limits_{\theta, \psi, \Upsilon} & \Upsilon \\ \text{subject to} & \\ \Upsilon \geq -\mathcal{A}\left(\theta^i, \psi^i\right) & \\ -\nabla\mathcal{A}\left(\theta^i, \psi^i\right)\binom{\psi-\psi^i}{\theta-\theta^i} & \\ \beta_{C1-Cv}\left(\theta^i, \psi^i\right) & \\ -\nabla\beta_{C1-Cv}\left(\theta^i, \psi^i\right)\binom{\psi-\psi^i}{\theta-\theta^i} \leq 0 \end{cases}$
Lower Bound $\leftarrow \Upsilon$
if Upper Bound − Lower Bound $\leq \epsilon$ **then**
$Convergence \leftarrow TRUE$
else
$i \leftarrow i + 1$
$\theta^i \leftarrow \theta^*$
end if
end while

The challenge described in Eq. (35) is revised and showcased in the form of Eq. (36).

$$\min_{\theta} \quad -\Upsilon(\theta)$$

such that:

$$\Upsilon(\theta) = \min_{\psi} \quad -\mathcal{A}\left(\theta^i, \psi\right) \tag{36}$$

subject to

$$\beta_{C1-Cv}\left(\theta^i, \psi\right) \leq 0$$

Equation (36) stands as the projection of Eqs. (29), (31), and (33) onto the τ space. Equation (34), representing the primal problem, guarantees the fulfillment of all constraints for each value of θ^i. The solution extracted from the projection problem is identified as Eq. (37).

$$\min_{\beta} \min_{\psi} \quad -\mathcal{A}\left(\theta^i, \psi^i\right) - \nabla\mathcal{A}\left(\theta^i, \psi^i\right)\begin{pmatrix}\psi - \psi^i \\ \theta - \theta^i\end{pmatrix}$$

subject to (37)

$$\beta_{C1-Cv}\left(\theta^i, \psi^i\right) - \nabla\beta_{C1-Cv}\left(\theta^i, \psi^i\right)\begin{pmatrix}\psi - \psi^i \\ \theta - \theta^i\end{pmatrix} \leq 0$$

The task of minimizing can be reformulated through the introduction of a novel variable Υ, as illustrated in eq. (38).

$$\min_{\beta,\psi,\Upsilon} \ \Upsilon$$

subject to

$$\Upsilon \geq -\mathcal{A}\left(\theta^i, \psi^i\right) - \nabla\mathcal{A}\left(\theta^i, \psi^i\right)\begin{pmatrix}\psi - \psi^i \\ \theta - \theta^i\end{pmatrix} \tag{38}$$

$$\beta_{C1-Cv}\left(\theta^i, \psi^i\right) - \nabla\beta_{C1-Cv}\left(\theta^i, \psi^i\right)\begin{pmatrix}\psi - \psi^i \\ \theta - \theta^i\end{pmatrix} \leq 0$$

The master problem, as presented in Eq. (38), serves the purpose of establishing the lower bound values. This master problem is tantamount to the original issues delineated in eqs. (29), (31), and (33), subject to the stipulation that propositions 1, 2, and 3 are satisfied for the master problem articulated in Eq. (38). To effectively address the mixed-integer linear programming (MILP) predicament outlined in Eq. (38), an iterative method termed the branch and bound algorithm is implemented [57].

3.1 Algorithm convergence and optimality

The OAA algorithm showcases a linear convergence rate, a fact supported by existing literature on mixed-integer programming [56]. The incorporation of the branch and bound framework empowers the ϵ-optimal OAA approach to attain nearly optimal outcomes, attaining a precision of $\epsilon = 10^{-3}$. Throughout the procedure, the discrete values of θ remain constant, and the OAA algorithm concludes with an optimal solution reached within a finite number of iterations, contingent on the satisfaction of all mentioned conditions and the confinement of the number of discrete variables θ. The ϵ-optimal algorithm ensures a solution within a range of ϵ from the optimal solution for any $\epsilon > 0$. Reducing the value of ϵ leads to more precise solutions. The optimality of ψ within the master problem hinges on the specific selection of discrete variables θ^i.

- A workable solution is realized when $\Upsilon \geq -\mathcal{A}\left(\theta^i, \psi^i\right)$.
- A solution is considered infeasible when $\Upsilon \leq -\mathcal{A}\left(\theta^i, \psi^i\right)$.

The objective of the algorithm is to secure convergence by discarding infeasible solutions for the master problem, thereby guaranteeing finite convergence. Although the algorithm ascertains optimality for constant θ values due to the convex nature of both the objective and constraint functions, the escalating computational burden of the ESA curtails its feasibility in practical scenarios. The complexity of ESA can be denoted as $\mathcal{C}^{ESA}$ and computed using Eq. (39) [52].

$$\mathcal{C}^{ESA} = 2^{|i|} \tag{39}$$

Nonetheless, leveraging the OAA methodology enables the acquisition of an ϵ-optimal outcome within a defined number of iterations [53]. The computational intricacy of the OAA, denoted as $\mathcal{C}^{OAA}$, can be computed using Eq. (40), resulting in a more feasible computational load when compared to algorithms that provide precise solutions.

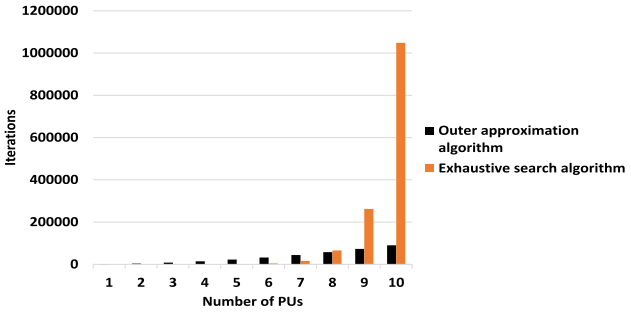

Fig. 2 Computational complexity of outer approximation algorithm and exhaustive search algorithm versus number of PUs

$$\mathcal{C}^{OAA} = \frac{i^2\kappa}{\lambda} \tag{40}$$

OAA ensures an ϵ-optimal outcome within a designated error threshold λ relative to the worldwide optimal solution, positioning it as a superior alternative to ESA. The constraints denoted as κ are actively incorporated in the optimization procedure. Figure 2 visually demonstrates the computational intricacy pattern of both OAA and ESA.

3.2 Complexity of ϵ-optimal algorithm

This section furnishes a comprehensive analysis of the complexity inherent in the proposed algorithm. The intricacy is gauged by quantifying the number of floating-point operations (flops) demanded by various procedures encompassing simple addition, complex addition, elementary multiplication, intricate multiplication, division, set operations, matrix multiplications, assignment operators, and logical operators. Every mathematical operation incurs a specific tally of flops, with fundamental actions like addition, multiplication, and division incurring one flop each. More intricate actions such as complex addition and complex multiplication necessitate two and four flops, correspondingly. The inclusion or exclusion of an element from a set entails one flop. Matrix multiplications involving matrices of dimensions $e \times f$ and $f \times y$ contribute a total of $2efy$ flops. Both assignment operators and logical operators each contribute one flop. This meticulous analysis of complexity affords valuable insights into the algorithm's computational efficiency.

The complexity of the proposed algorithm is gauged through specific guidelines. The initialization phase of the algorithm contributes 5 flops. Solving the NLP problem and obtaining the upper bound of the optimal solution entails $2NCB$ flops, whereas the computation of the MILP problem

and acquisition of the lower bound of the optimal solution necessitates $4NCB\beta$ flops. The comparison between the lower and upper bounds adds 2 flops. The introduction of fresh binary variables introduces 4 flops. The comprehensive complexity of the algorithm is defined by the cumulative flops count F, as exemplified by Eq. (41). This complexity analysis yields valuable insights into the algorithm's computational demands.

$$\begin{aligned} F_{OAA} &= 5 + 2NCB + 4NCB\beta + 4NCB\beta + 2NCB\beta + 4 \\ F_{OAA} &= 9 + 2NCB + 10NCB\beta \\ F_{OAA} &\approx 2NCB + 10NCB\beta \end{aligned} \tag{41}$$

The computational intricacy of the ϵ-optimal OAA technique can be concisely characterized using Big O notation as O(N $\times$C$\times$ B) + O(N $\times$C $\times$ B $\times$ β), where N signifies the number of PUs, C denotes the number of MCCs, SCCs, or UAVCs, B represents the count of cells, and β refers to the constraints. This complexity analysis furnishes an approximation of the computational resources demanded by the OAA algorithm contingent on the dimensions of the specific problem instance.

3.3 Proposed strategy for future scope of 6G networks

3.3.1 Factors involved in the proposed strategy to determine the size and composition of PU clusters

In determining the size and composition of PU clusters to maximize throughput and EE within the given scenario, factors such as geographical distribution and density of PUs play a crucial role, influencing the formation of clusters based on channel gain values. The dynamic nature of PU traffic and channel conditions should be accounted for, enabling adaptive clustering to accommodate varying demand patterns. The integration of SC and UAV introduces additional dimensions to cluster composition, necessitating careful consideration of the network infrastructure's capabilities and the EE benefits offered by UAV. Channel gain-based PUC, guided by precise CSI, enables the formation of clusters like MCCs, SCCs, and UAVCs. Dynamic adjustment of cluster sizes based on real-time channel conditions and PU distributions is essential [58, 59]. Additionally, the allocation of subcarriers using a H-MA approach and the integration of energy-efficient UAV contribute to optimizing throughput and EE. The network should adaptively balance cluster sizes, leveraging accurate information on channel gain values and channel states, to ensure efficient downlink communication across diverse network scenarios. Furthermore, effective resource allocation, such as the use of OMA and NOMA based on the number of PUs in a cluster, is essential for optimizing both throughput and EE.

3.3.2 Proposed strategy with power control mechanism and sleep scheduling algorithms

With the proposed strategy, the power control mechanisms and sleep scheduling algorithms play pivotal roles in achieving overall energy savings in 6G networks. Power control mechanisms dynamically adjust transmit power levels based on real-time channel conditions and PU requirements, optimizing energy usage [60]. Sleep scheduling algorithms strategically deactivate certain network components during periods of low demand, reducing idle power consumption [61]. By synchronizing sleep schedules with PU activity patterns and leveraging advanced power management strategies, the method aims to achieve significant EE gains in the 6G network, ensuring optimal resource utilization and environmental sustainability [62].

3.3.3 Proposed strategy with machine learning algorithms

By analyzing historical data and PU patterns, machine learning models can anticipate PU behaviors and adaptively adjust resource allocations in real-time. This enables the network to dynamically allocate resources based on predicted PU demands, optimizing throughput, and minimizing energy consumption. The integration of machine learning algorithms in the resource allocation process enhances the network's ability to proactively respond to changing PU needs, contributing to the overall efficiency and performance in terms of both throughput and energy consumption [63, 64].

3.3.4 Influence of proposed strategy with UAV's altitude, mobility, and deployment strategy

The overall performance of downlink communication is significantly influenced by the UAV's altitude, mobility, and deployment strategy. The UAV's altitude plays a crucial role in coverage and signal strength, affecting the communication range, potential interference and quality [65]. UAV mobility influences adaptability to changing network conditions, allowing for dynamic positioning to optimize coverage and serve PUC efficiently, impacts the UAV's ability to dynamically adapt to varying PU demands [66]. The deployment strategy, encompassing the location of deployed UAV, determines the UAV's effectiveness in serving specific areas or clusters of PUs, which directly impacts the overall network coverage and capacity [67]. By carefully adjusting these parameters, the UAV can enhance coverage, throughput, and EE, ensuring the effectiveness of overall performance of downlink communication.

Table 5 Input parameters

Parameters	Values
d_o	10 m
G_o	50
α	2
ξ	10 dB
Minimum PUs	20
PUs Increment	20
Maximum PUs	100
PUs Distribution	Uniform
R^n_{min}	{0.5, 1.5, 2.5, , 3.5} Mbps
MC Coverage	1000 m
SC Coverage	500 m
UAV Coverage	300 m
Minimum transmit power	12 dBm
Maximum transmit power	60 dBm

4 Results and discussions

This paper conducts a comprehensive evaluation of the introduced method, which entails PUC-based downlink H-MA, across various network paradigms, encompassing MC-only networks, HetNets, and UAV-assisted HetNets. The newly formulated MINLP problem instances elucidated in Eqs. (29), (31), and (33), grounded in innovative network models depicted in Fig. 1a, b, and c, are effectively solved utilizing the OAA approach. The performance scrutiny of the proposed methodology within these diverse networks encompasses an analysis of crucial PIs, including PU admission, association, PUFAC, network achieved throughput, and EE. Moreover, a comparative assessment of the method's performance is conducted across all network categories and also with the existing most related work in [21] to validate our theoretical work. To implement the ϵ-optimal OAA technique, a basic open-source non-linear mixed-integer programming (BONMIN) solver is employed [57].

Table 5 presents a comprehensive overview of the input parameters harnessed in this study. The lower limit for the count of PUs is initialized at 20, escalating incrementally by 20 PUs until reaching the permissible maximum of 100 PUs. The utmost coverage spans are delineated as 1000 m for HC, 500 m for SC, and 300 m for UAV. The antenna gain G_o is established at 50, alongside a shadowing Gaussian random variable ξ amounting to 10 dB, a path loss exponent α set to 2, and a far-field reference distance d_o established at 10 m. Cells are postulated to possess a minimum transmission power of 12 dBm and a maximum transmission power of 50 dBm. For the PUs, the minimum QoS R^n_{min} is diversified across {0.5, 1.5, 2.5, 3.5} Mbps.

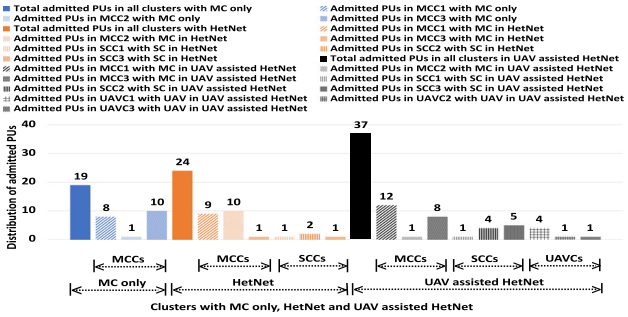

Fig. 3 Admitted PUs distribution in clusters in MC only network, HetNet, and UAV assisted HetNet

Figure 3 depicts the dispersion of admitted PUs within clusters, encompassing MCCs coupled with MC in MC-only networks, MCCs coupled with MC, SCCs linked with SC in HetNets, and MCCs coupled with MC, SCCs linked with SC, UAVCs coordinated with UAV in UAV-assisted HetNets, where the total number of PUs considered are 40. The illustration notably reveals that the aggregate of PUs admitted within UAV-assisted HetNet clusters surpasses that of both conventional MC-only networks and HetNets. This prevalence arises from the inherent benefits facilitated by UAVs in HetNets. UAVs, functioning as aerial base stations effectively extending coverage in regions characterized by coverage gaps or heightened PU concentrations. Furthermore, the admission of solitary PU within any cluster entails the utilization of OMA, whereas the admission of multiple PUs within a cluster entails the employment of NOMA. The conjoined application of both techniques culminates in the deployment of H-MA.

Illustrated in Fig. 4 is the trajectory of the cumulative admitted PUs across all clusters in MC-only networks, HetNets, and UAV-assisted HetNets, while progressively augmenting the count of PUs in each network from 20 to 100, with intervals of 40. The cumulative admitted PUs exhibit an upward trend in all cluster configurations, spanning MC-only networks, HetNets, and UAV-assisted HetNets, aligning with the escalation in the number of PUs. Notably, the proposed methodology employed within UAV-assisted HetNets emerges as superior in terms of cumulative admitted PUs within clusters, compared to other network configurations. In MC-only networks, there exists a likelihood of capacity saturation, resulting in a restricted number of PUs accommodated due to resource limitations and potential congestion. In HetNets integrating both MC and SC, the added capacity from SCs could alleviate congestion, permitting an enhanced PU count, albeit the introduction of interference amid distinct cell types might impede performance. In contrast, UAV-assisted HetNets harness the attributes of UAVs, enabling potentially higher PU admission rates, as UAVs can match demand and optimize coverage.

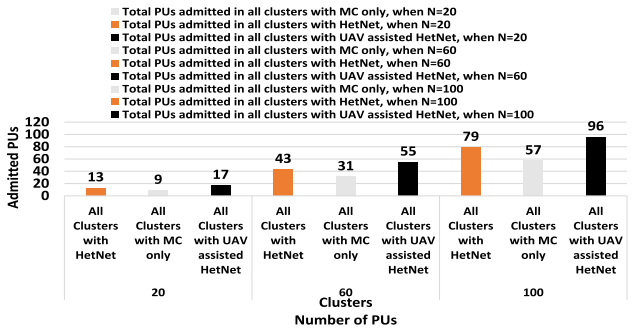

Fig. 4 Total PUs admitted in all clusters versus number of PUs in MC only network, HetNet, and UAV assisted HetNet

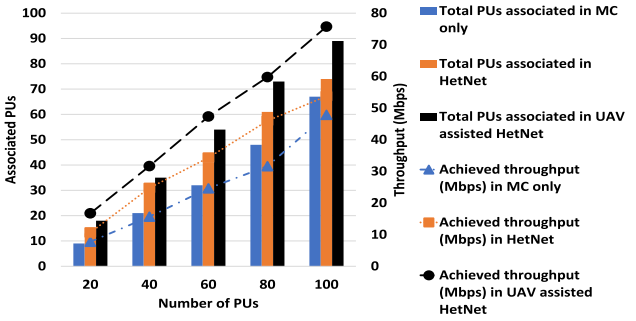

Fig. 5 Associated PUs and throughput (Mbps) versus number of PUs in MC only network, HetNet, and UAV assisted HetNet

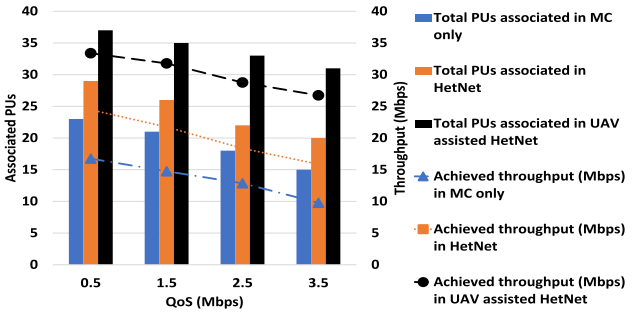

Fig. 6 Associated PUs and throughput (Mbps) versus required QoS (Mbps) in MC only network, HetNet, and UAV assisted HetNet

Displayed in Fig. 5 is the evolving trend of affiliated PUs and throughput (in Mbps) juxtaposed against the increasing number of PUs within MC-only networks, HetNets, and UAV-assisted HetNets. With the progressive augmentation of PUs in these network configurations, both affiliated PUs and throughput exhibit an ascending trajectory, primarily attributed to augmented resource exploitation and extended network coverage. Within MC-only networks, the allocation of resources becomes more efficient as the PU count escalates, enabling the accommodation of additional PUs. In the realm of HetNets, characterized by the integration of MC and SC, elevated capacity ensues from SCs alleviating traffic from MC, thereby fostering heightened PU association and subsequent throughput. In UAV-assisted HetNets, the adaptable deployment of UAV cells optimizes both coverage and capacity, proficiently absorbing a larger number of PUs within regions marked by heightened demand or coverage voids. Notably, the proposed technique within UAV-assisted HetNets outperforms its counterparts in terms of affiliated PUs and throughput as PU numbers surge. This superiority can be attributed to the effectiveness of H-MA in managing interference and harnessing multiplexing gains. This orchestration results in the judicious utilization of resources, escalated PU capacity, augmented throughput, and an increased tally of associated PUs as PU numbers expand. Consequently, this technique emerges as a robust solution for enhancing network performance within scenarios featuring burgeoning PU populations.

Illustrated in Fig. 6 is the trajectory of affiliated PUs and throughput (in Mbps) in correlation with escalating required QoS (in Mbps) across MC-only networks, HetNets, and UAV-assisted HetNets. As the requisitioned QoS of PUs amplifies within these network contexts, a characteristic decline is observed in both affiliated PUs and throughput. This diminution can be attributed to the intensified resource demands that ensue. In MC-only networks, the augmented QoS prerequisites engender resource scarcity, culminating in the curtailment of the PU count that can be serviced at the stipulated QoS. Analogously, HetNets grapple with analogous challenges, wherein augmented QoS requisites strain resources, adversely affecting the performance of both MC and SC. This, in turn, begets a reduction in PU association and throughput. Within UAV-assisted HetNets, escalated QoS requisites can impose resource allocations that may prove untenable, primarily due to energy constraints inherent to UAVs. However, intriguingly, the proposed technique within UAV-assisted HetNets excels in terms of affiliated PUs and throughput in the face of heightened required QoS. This commendable performance is rooted in H-MA's adept allocation of resources and effective interference mitigation. Consequently, an improved resource utilization are achieved, culminating in a superior performance concerning affiliated PUs and throughput as the requisitioned QoS escalates. This endorses H-MA as a robust strategy for adeptly addressing escalating QoS demands within network contexts.

Depicted in Fig. 7 is the trajectory of throughput (in Mbps) and EE (in Mbps/Watts) as a function of escalating PU numbers across MC-only networks, HetNets, and UAV-assisted HetNets. The observed trend reflects an upward trajectory of both throughput and EE, as the PU count increases. This augmentation is underpinned by heightened resource utilization and network densification. In MC-only networks, an augmented PU population stimulates a more efficient exploitation of available resources. Within HetNets, the synergy of both MC and SC fosters an equitable distribution of traffic, thereby engendering an upswing in both through-

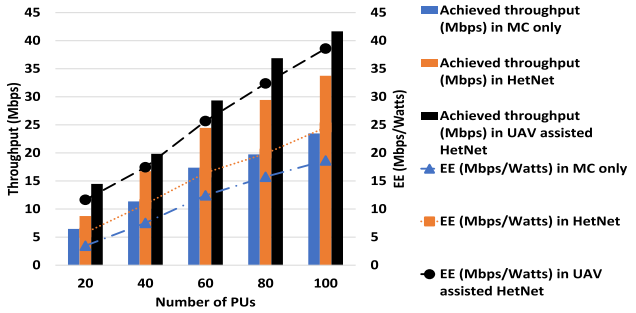

Fig. 7 Throughput (Mbps) and EE (Mbps/Watts) versus number of PUs in MC only network, HetNet, and UAV assisted HetNet

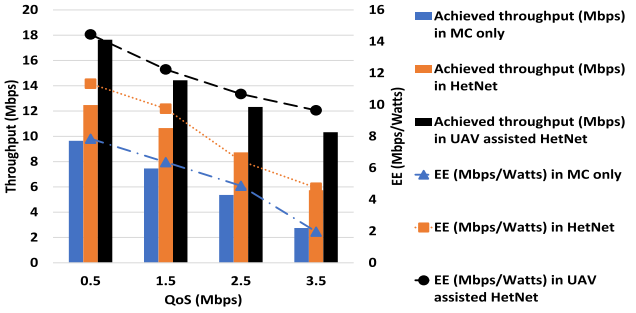

Fig. 8 Throughput (Mbps) and EE (Mbps/Watts) versus required QoS (Mbps) in MC only network, HetNet, and UAV assisted HetNet

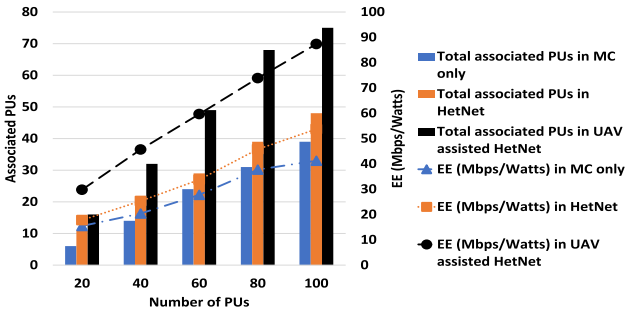

Fig. 9 Associated PUs and EE (Mbps/Watts) versus number of PUs in MC only network, HetNet, and UAV assisted HetNet

put and EE. In the context of UAV-assisted HetNets, the strategic deployment of UAVs enables targeted coverage enhancement in zones characterized by elevated PU demand. Notably, the proposed technique within UAV-assisted HetNets serves to accentuate these advantages by orchestrating interference management and capitalizing on multiplexing gain. This yields a resource allocation mechanism that optimizes power utilization and fosters the judicious use of available resources. As a result, with the elevation of PU numbers, the PUC approach rooted in H-MA contributes to a heightened throughput and EE. This effect is attributed to the intelligent resource allocation and interference minimization tactics, which collectively culminate in a comprehensive amelioration of network performance.

Illustrated in Fig. 8 is the pattern of throughput (in Mbps) and EE (in Mbps/Watts) concerning the intensification of required QoS (in Mbps) within MC-only networks, HetNets, and UAV-assisted HetNets. An evident decline in both throughput and EE is observable across these network paradigms as the requisitioned QoS of PUs escalates. This phenomenon is underpinned by an aggravated resource competition and the challenges of complying with exacting QoS demands. In the realm of MC-only networks, heightened QoS prerequisites can precipitate congestion and resource scarcity, thereby curbing overall throughput and EE. Akin dilemmas plague HetNets, where amplified QoS mandates strain resources across both MC and SC, engendering a reduction in both throughput and EE. Within the domain of UAV-assisted HetNets, the act of elevating QoS requisites may pose limitations in resource allocation due to the constraints tied to UAV energy. Nevertheless, the proposed technique within UAV-assisted HetNets prevails in terms of throughput and EE amidst mounting QoS demands. By effectively managing interference and resource allocation, the H-MA approach orchestrates optimized resource utilization, thereby fostering the amelioration of both throughput and EE even in the face of more exacting QoS conditions. This underscores the efficacy of the H-MA strategy as a potent means of upholding network performance amid escalating QoS stipulations.

As depicted in Fig. 9, the progression of associated PUs and EE (in Mbps/Watts) against the backdrop of an escalating number of PUs unfolds across MC-only networks, HetNets, and UAV-assisted HetNets. In each of these network configurations, a surge in the number of PUs yields a concurrent rise in associated PUs and EE. This phenomenon is a consequence of the intensified resource distribution and network densification engendered by an expanded PU population. In the realm of MC-only networks, the greater influx of PUs facilitates more judicious resource allocation, thereby bolstering both associated PUs and EE. The integration of MC and SC within HetNets further augments this trend as it optimizes the allocation of traffic, resulting in elevated levels of associated PUs and EE. In UAV-assisted HetNets, the dynamic deployment of UAVs targets areas with heightened PU demand, thereby optimizing network coverage and capacity. Notably, the proposed technique harnessed within UAV-assisted HetNets not only enhances this trajectory but also accentuates it. By adroitly managing interference and capitalizing on multiplexing gain, the approach facilitates superior resource allocation, ultimately fostering an augmentation of both associated PUs and EE. This efficacy is particularly pronounced as the number of PUs surges, thereby solidifying the H-MA-based PUC strategy as a pivotal instrument for elevating network performance.

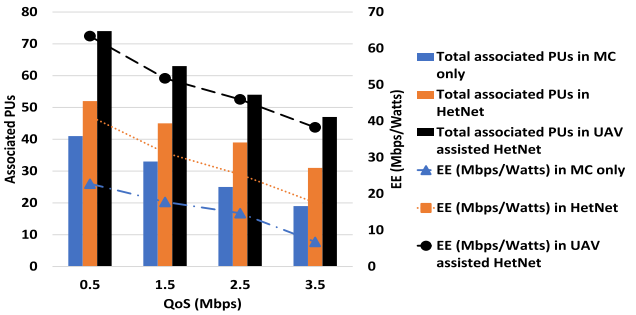

Fig. 10 Associated PUs and EE (Mbps/Watts) versus required QoS (Mbps) in MC only network, HetNet, and UAV assisted HetNet

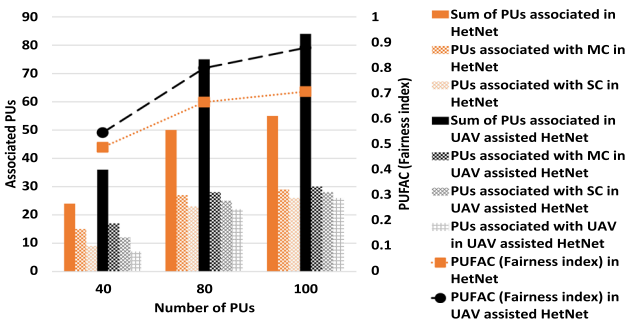

Fig. 11 Associated PUs and PUFAC (fairness index) versus number of PUs in HetNet, and UAV assisted HetNet

As depicted in Fig. 10, the trajectory of associated PUs and EE (in Mbps/Watts) unfolds in response to escalating required QoS (in Mbps) across MC-only networks, HetNets, and UAV-assisted HetNets. Across these diverse network configurations, a discernible pattern emerges: associated PUs and EE tend to decline as the stipulated QoS for PUs surges. This downward trend can be attributed to the exacerbation of resource contention and the inherent challenges of meeting more stringent QoS demands. Within MC-only networks, where elevated QoS requirements are encountered, the consequence is often a surge in congestion and resource scarcity, culminating in a reduction of associated PUs and EE. Analogously, the challenges faced by HetNets, encompassing both MC and SC, are compounded as higher QoS mandates strain resources across both types of cells, thereby curbing the performance metrics. However, the strategy proposed for UAV-assisted HetNets distinguishes itself by effectively navigating interference and optimizing the allocation of resources. This adept management ensures the judicious use of resources, thereby engendering an enhancement in both associated PUs and EE, even under conditions of heightened QoS requisites. Consequently, as the imperative for higher QoS among PUs gains prominence, the efficacy of the H-MA-based PUC strategy becomes increasingly apparent, solidifying its position as a potent approach in addressing the challenges posed by more demanding QoS expectations.

As illustrated in Fig. 11, the progression of associated PUs and PUFAC (fairness index) unfolds in parallel with the escalation of PU numbers within HetNets, and UAV-assisted HetNets. This observable rise in associated PUs and an enhanced fairness index can be ascribed to the adept allocation of resources and the augmentation of network density. This upward trajectory finds its foundation in the efficient distribution of traffic and the optimization of coverage. The proposed technique deployed within UAV-assisted HetNets magnifies this impact by adroitly managing interference and optimizing the effective utilization of resources, culminating in a more balanced distribution of PU associations and the equitable apportioning of resources. As the number of PUs continues to climb, the proficiency of the H-MA-based PUC approach in navigating interference becomes increasingly evident, contributing to an escalation in associated PUs and a heightened fairness index. This robustness underscores its efficacy in maintaining networks that are both equitable and high-performing, even in the face of mounting PU demands.

As depicted in Fig. 12, the distribution pattern of associated PUs and PUFAC (fairness index) in relation to the required QoS (Mbps) unfolds distinctly across HetNets and UAV-assisted HetNets. As the stipulated QoS expectations for PUs are heightened, a notable decrease in associated PUs transpires, concurrently with an improvement in the PUFAC (fairness index). This trend is rooted in the imposition of resource limitations due to the augmented QoS requisites, leading to the potential inability of certain PUs to fulfill the stringent criteria. Consequently, there is a decline in the count of associated PUs. However, the proposed technique within UAV-assisted HetNets counters this trend through its adept management of interference and optimization of resource allocation. This strategic approach culminates in the enhancement of the equitable dissemination of resources, thus yielding an augmentation in both associated PUs and the fairness index in the realm of PU association. As the QoS requirements for PUs surge, the H-MA-based PUC's proficiency in interference management takes center stage, orchestrating an elevation in associated PUs and a commendable advancement in fairness effectively establishing it as a potent strategy to uphold network performance amid escalating QoS demands.

Illustrated in Fig. 13, the dispersion pattern of EE (Mbps/Watts) and PUFAC (fairness index) as a function of the number of PUs unfolds distinctly across HetNets and UAV-assisted HetNets. As the PU count escalates in both HetNets and UAV-assisted HetNets, a discernible escalation in EE (Mbps/Watts) ensues, accompanied by a notable enhancement in the PUFAC (fairness index). This phenomenon is attributed to the heightened density of PUs, a factor that facilitates more efficient resource sharing and utilization. In this context, the proposed technique deployed within UAV-

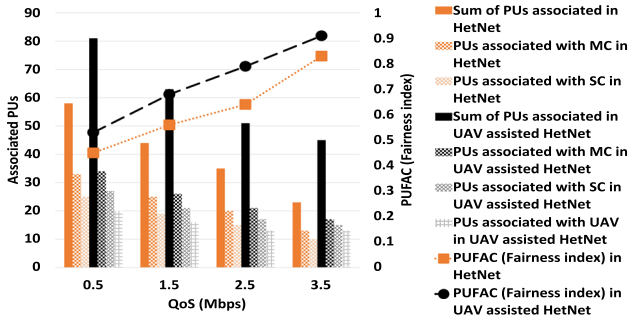

Fig. 12 Associated PUs and PUFAC (fairness index) versus number of PUs in HetNet, and UAV assisted HetNet

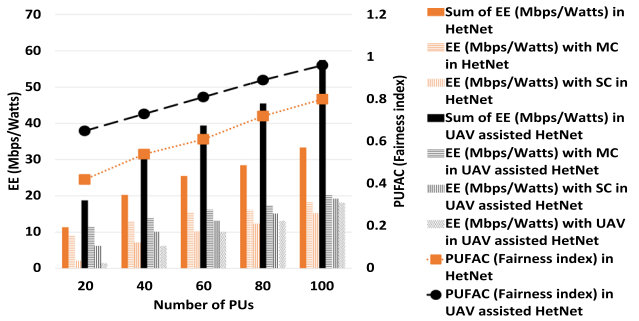

Fig. 13 EE (Mbps/Watts) and PUFAC (fairness index) versus number of PUs in HetNet, and UAV assisted HetNet

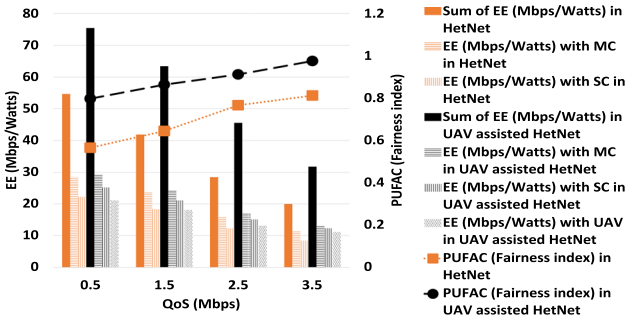

Fig. 14 EE (Mbps/Watts) and PUFAC (fairness index) versus required QoS (Mbps) in HetNet, and UAV assisted HetNet

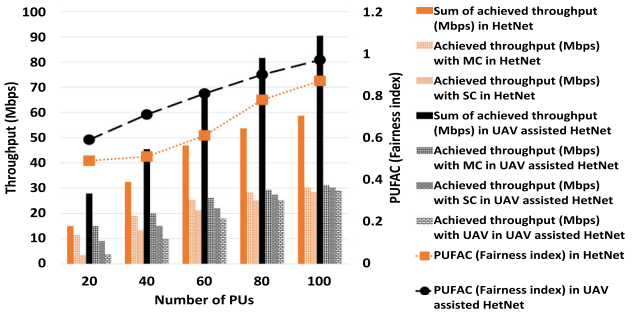

Fig. 15 Throughput (Mbps) and PUFAC (fairness index) versus number of PUs in HetNet, and UAV assisted HetNet

assisted HetNets excels by adroitly navigating interference and optimizing the allocation of resources. This strategic maneuvering culminates in a refined resource utilization, which in turn accentuates EE (Mbps/Watts) and engenders a more balanced PU fair association. The culmination of these effects underscores the potency of the downlink H-MA-based PUC strategy in sustaining network performance in the face of an expanding number of PUs.

Depicted in Fig. 14, the portrayal of the correlation between EE (Mbps/Watts) and PUFAC (fairness index) in relation to the requisite QoS (Mbps) offers distinct insights across HetNets and UAV-assisted HetNets. As the demand for elevated QoS from PUs rises in both network configurations, a notable decline in EE (Mbps/Watts) becomes apparent, accompanied by a discernible enhancement in PUFAC (fairness index). This phenomenon is primarily attributed to the intensified resource contention and the constraints posed by the fulfillment of stringent QoS requisites. Notwithstanding this challenge, the proposed technique in UAV-assisted HetNets adeptly counteracts this trend by adroitly managing interference and optimizing the allocation of resources. This strategic maneuver culminates in an elevated judicious resource utilization, translating into a discernible improvement in EE (Mbps/Watts) and a more balanced PU fair association. This underlines the efficacy of the H-MA-based PUC strategy in upholding network performance, even as the network contends with the escalating demands for enhanced QoS provisioning.

Figure 15 shows the distribution trend of throughput (Mbps) and PUFAC (fairness index) versus number of PUs in HetNet, and UAV assisted HetNet. The augmentation of the PU count in HetNets and UAV-assisted HetNets yields amplified throughput and an enhanced PUFAC (fairness index), a phenomenon stemming from improved resource utilization and network densification. Notably, the proposed technique in UAV-assisted HetNets outperforms its counterparts in terms of both throughput and fairness index as the PU count escalates. This pronounced effectiveness is attributed to its adept management of interference and optimized resource allocation. Through these mechanisms, the strategy optimizes resource utilization, culminating in elevated throughput and a more equitably distributed PU fair association. As a result, the H-MA-based PUC strategy emerges as a robust approach for sustaining network performance within contexts characterized by a burgeoning number of PUs.

Illustrated in Fig. 16, is the distribution trend of throughput (Mbps) and PUFAC (fairness index) concerning the required QoS (Mbps) within MC-only networks, HetNets, and UAV-assisted HetNets. As the demanded QoS for PUs escalates in HetNets and UAV-assisted HetNets, a reduction in throughput is observed, while concurrently witnessing an enhancement in PUFAC (fairness index), mainly due to the

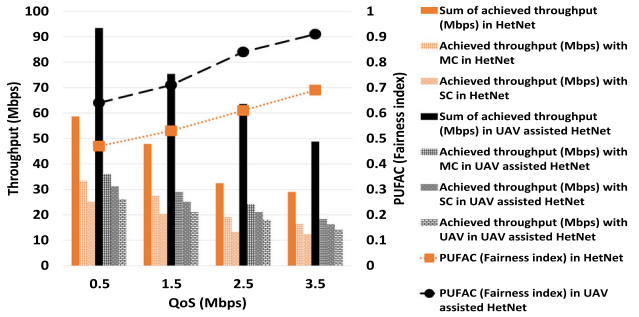

Fig. 16 Throughput (Mbps) and PUFAC (fairness index) versus required QoS (Mbps) in HetNet, and UAV assisted HetNet

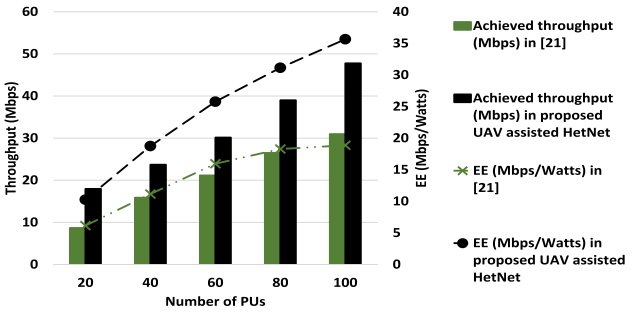

Fig. 17 Comparing the proposed strategy of this paper in UAV assisted HetNet with the strategy proposed in [21] regarding throughput (Mbps) and EE (Mbps) versus number of PUs

imposition of stringent QoS criteria that engender resource contention. Nevertheless, the proposed technique within UAV-assisted HetNets offsets this throughput decrease via proficient interference management and optimal resource allocation. This approach engenders an augmented resource utilization, ultimately contributing to amplified throughput and an equitable distribution of PU fair association. As the demanded QoS of PUs ascends, the proficiency of H-MA-based PUC in managing interference results in augmented throughput and an elevated fairness index in PU association, underscoring its effectiveness in maintaining network performance amid exacting QoS requisites.

A comparison of the proposed strategy in this paper with the existing work in [21] is presented in Fig. 17 that shows the behavior of throughput (Mbps) and EE (Mbps/Watts) as a function of increasing number of PUs. It has been observed that both throughput and EE increase for the proposed strategy in UAV-assisted HetNet and the technique used in [21] as the number of PUs increases. This enhancement is supported by increased resource efficiency and network densification. In [21], employing NOMA within HetNets, the collaboration of both MC and SC promotes a balanced distribution of traffic, consequently leading to an increase in both throughput and EE. However, in our paper, the tactical deployment of UAVs facilitates targeted coverage improvement in areas characterized by heightened PU demand in UAV-assisted HetNet. Notably, in [21], when the number of PUs increases from 80 to 100, throughput increases, and EE stabilizes because the network reaches its maximum capacity, and a further increase in the number of PUs will result in decreased EE. Compared to that, in this work, both throughput and EE increase when the number of PUs increases in the network because the PUC prevents PUs from inter-cluster interference that results in increased throughput and EE. Additionally, the low-powered UAV provides coverage to those areas where HetNet cannot provide ultimately increasing PU association, resulting in increased throughput and EE. Overall, it shows the superior performance of the proposed strategy in the UAV-assisted HetNet in our paper than the strategy used in [21].

5 Conclusions and future directions

This research introduces an innovative approach that involves the integration of PUC with downlink H-MA techniques within UAV-assisted HetNets, aimed at collectively optimizing PU admission within clusters, cell associations, network throughput, and EE while maintaining fairness. The resolution of this intricate MINLP challenge is accomplished through the implementation of an OAA. The efficacy of this proposed methodology within UAV-assisted HetNets is evaluated and juxtaposed with the MC-only network and HetNet scenarios currently in place. In addition to this, the performance of the proposed strategy in UAV assisted HetNet is compared with the strategy used in [21]. The outcomes of this evaluation underscore the superior performance of UAV-assisted HetNets compared to both the MC-only network and HetNets, as evidenced by various PIs such as the maximization of throughput, EE, PU admission in clusters, PU-cell associations, power allocation for PUs, and PUFAC. Also, outcomes of the comparison of the proposed strategy in UAV assisted HetNet with the work done in [21] underscore the superior performance of UAV-assisted HetNets compared to work in [21], as evidenced by various PIs such as the maximization of throughput, EE, for increasing number of PUs, and this comparison validates our work.

The results clearly demonstrate the newfound strategy's heightened efficacy within UAV-assisted HetNets when contrasted with both MC-only networks and HetNets and work done in [21]. This superiority can be attributed to the expanded coverage and enhanced connectivity achieved through the integration of MC, SC, and UAV technologies for the PUs, ultimately contributing to improved throughput and EE. These notable findings emphasize the viability of the proposed approach as a strong contender for incorporation into upcoming 6G networks. Furthermore, there's potential for

future exploration by applying this technique to visible light communication (VLC) networks, considering more practical scenarios to expand its applicability.

Author Contributions A author wrote main manuscript, prepared figures, and conduct simulations. A and B authors reviewed the manuscript.

Funding The authors have not disclosed any funding.

Declarations

Conflict of interest The authors declare no competing interests.

Appendix A

Fractional programing and Charnes Cooper transformation

Fractional programme (FP) contains objective function as a ratio of two nonlinear functions generally. A FP is defined as

$$\max_{t \in S} \frac{j(t)}{k(t)} \quad \text{subject to} \quad C1 : g_n(t) \leq 0 \tag{42}$$

where $j(t)$, $k(t)$ and $g_n(t)$ (where $n = 1, 2, ..., N$) are defined on set $S \subset R^t$, having real values. In (42), if $j(t)$ is positive and concave, $k(t)$ is positive and convex, assuming S is convex set, then FP is called CFP. CCT [68] use following variable transformations to reduce a CFP to a concave programme.

$$w = \frac{t}{k(t)} \tag{43}$$

$$z = \frac{1}{k(t)} \tag{44}$$

The equivalent concave problem for (42) can be written as

$$\max_{\frac{w}{z} \in S} z j_o \frac{w}{z}$$

subject to

$$C1 : zk(\frac{w}{z}) = 1, \qquad C2 : zg_n(\frac{w}{z}) \leq 0, \forall\ n = 1, 2, 3, ..., N. \tag{45}$$

Problem in (42) can have optimal solution if and only if problem in (45) have optimal solution.

References

1. López-Pérez, D., De Domenico, A., Piovesan, N., Xinli, G., Bao, H., Qitao, S., & Debbah, M. (2022). A survey on 5g radio access network energy efficiency: Massive mimo, lean carrier design, sleep modes, and machine learning. *IEEE Communications Surveys & Tutorials, 24*(1), 653–697.
2. Larsen, L. M., Christiansen, H. L., Ruepp, S., & Berger, M. S. (2023). Toward greener 5G and beyond radio access networks-a survey. *IEEE Open Journal of the Communications Society, 4*, 768–797.
3. Khanh, Q. V., Chehri, A., Quy, N. M., Han, N. D., & Ban, N. T. (2023). "Innovative trends in the 6g era: A comprehensive survey of architecture, applications, technologies, and challenges," *IEEE Access*.
4. Ansere, J. A., Kamal, M., Khan, I. A., & Aman, M. N. (2023). Dynamic resource optimization for energy-efficient 6G-IoT ecosystems. *Sensors, 23*(10), 4711.
5. Sundan, A. P., Jha, R. K., & Gupta, A. (2020). Energy and spectral efficiency optimization using probabilistic based spectrum slicing (PBSS) in different zones of 5G wireless communication network. *Telecommunication Systems, 73*(1), 59–73.
6. Beshley, M., Kryvinska, N., & Beshley, H. (2022). Energy-efficient GOE-driven radio resource management method for 5G and beyond networks. *IEEE Access, 10*, 131691–131710.
7. Gupta, A., & Jha, R. K. (2020). Power optimization with low complexity using scaled beamforming approach for a massive MIMO and small cell scenario. *Wireless Networks, 26*(2), 1165–1176.
8. Hmidi, K., Najeh, S., & Bouallegue, A. (2023). Power control approach in hetnets based-qlearning technique. In: International Wireless Communications and Mobile Computing (IWCMC). *IEEE, 2023*, 1184–1189.
9. Gupta, A., & Jha, R. K. (2017). Power optimization using optimal small cell arrangements in different deployment scenarios. *International Journal of Communication Systems, 30*(13), e3279.
10. Shen, L., Wang, N., Zhang, D., Chen, J., Mu, X., & Wong, K. M. (2022). Energy-aware dynamic trajectory planning for UAV-enabled data collection in MMTC networks. *IEEE Transactions on Green Communications and Networking, 6*(4), 1957–1971.
11. Jha, K., Gupta, A., Alabdulatif, A., Tanwar, S., Safirescu, C. O., & Mihaltan, T. C. (2022). CSVAG: Optimizing vertical handoff using hybrid cuckoo search and genetic algorithm-based approaches. *Sustainability, 14*(14), 8547.
12. Su, Y., Pang, X., Chen, S., Jiang, X., Zhao, N., & Yu, F. R. (2022). Spectrum and energy efficiency optimization in IRS-assisted UAV networks. *IEEE Transactions on Communications, 70*(10), 6489–6502.
13. Wu, Y., Liu, S., Lin, X., & Sun, L. (2023). Energy-efficiency optimization-based user selection and power allocation for uplink noma-enabled iot networks. In: *2023 IEEE 12th International Conference on Educational and Information Technology (ICEIT)*. IEEE, pp 321–325.
14. Ghafoor, U., Ali, M., Khan, H. Z., Siddiqui, A. M., Naeem, M., & Rashid, I., (2021). Energy efficiency optimization for hybrid noma based beyond 5g heterogeneous networks. In: IEEE 94th Vehicular Technology Conference (VTC2021-Fall). *IEEE, 2021*, pp. 1–5.
15. Jain, P., Gupta, A., Kumar, N., Joshi, G. P., & Cho, W. (2022). Performance evaluation of cooperative OMA and NOMA systems in 6g deployment scenarios. *Sensors, 22*(11), 3986.
16. Mukherjee, P., & De, T. (2023). Energy aware cluster head rotation for D2D multicasting. In: *2023 10th International Conference on Signal Processing and Integrated Networks (SPIN)*. IEEE, pp. 840–845.
17. Prasad, L. C., Kamatham, Y., Sunehra, D. (2022). An energy efficient fuzzy level clustering for stable communications in cogni-

tive sensor networks. In: *2022 International Conference on Smart Generation Computing, Communication and Networking (SMART GENCON)*. IEEE, pp. 1–6.
18. Zhang, T., Zhu, K., Wang, J., & Han, Z. (2021). Cost-efficient beam management and resource allocation in millimeter wave backhaul hetnets with hybrid energy supply. *IEEE Transactions on Wireless Communications, 21*(5), 3291–3306.
19. Beshley, M., Kryvinska, N., & Beshley, H. (2022). Energy-efficient GOE-driven radio resource management method for 5G and beyond networks. *IEEE Access, 10*, 131691–131710.
20. Qin, P., Fu, Y., Feng, X., Zhao, X., Wang, S., & Zhou, Z. (2021). Energy-efficient resource allocation for parked-cars-based cellular-v2v heterogeneous networks. *IEEE Internet of Things Journal, 9*(4), 3046–3061.
21. Xiao, H., Zhang, W., & Chronopoulos, A. T. (2022). Joint subchannel and power allocation for energy efficiency optimization in NOMA heterogeneous networks with energy harvesting. *IEEE Systems Journal, 16*(3), 4904–4915.
22. Fall, M., Balboul, Y., Fattah, M., Mazer, S., El Bekkali, M., & Kora, A. D. (2023). Towards sustainable 5G networks: A proposed coordination solution for macro and pico cells to optimize energy efficiency. *IEEE Access*.
23. Cao, Y., Wang, A., Sun, G., & Liu, L. (2023). Average transmission rate and energy efficiency optimization in uav-assisted IoT. In: . IEEE Wireless Communications and Networking Conference (WCNC). *IEEE, 2023*, pp. 1–6.
24. Oh, J., Lim, D.-w., Kang, K.-m. (2022). Energy efficiency improvement rate for low power UAV identification environment. In: *2022 13th International Conference on Information and Communication Technology Convergence (ICTC)*. IEEE, pp. 2139–2141.
25. Ma, X., Na, Z., Lin, B., & Liu, L. (2022). Energy efficiency optimization of uav-assisted wireless powered systems for dependable data collections in internet of things. *IEEE Transactions on Reliability*.
26. Shen, L., Wang, N., Zhang, D., Chen, J., Mu, X., & Wong, K. M. (2022). Energy-aware dynamic trajectory planning for UAV-enabled data collection in MMTC networks. *IEEE Transactions on Green Communications and Networking, 6*(4), 1957–1971.
27. Dai, X., Duo, B., Yuan, X., & Tang, W. (2022). Energy-efficient UAV communications: A generalized propulsion energy consumption model. *IEEE Wireless Communications Letters, 11*(10), 2150–2154.
28. Xiao, H., Jiang, H., Deng, L.-P., Luo, Y., & Zhang, Q.-Y. (2022). Outage energy efficiency maximization for UAV-assisted energy harvesting cognitive radio networks. *IEEE Sensors Journal, 22*(7), 7094–7105.
29. Baştürk, İ. (2021). Energy-efficiency maximization for multi-antenna ofdma networks. In: 29th Signal Processing and Communications Applications Conference (SIU). *IEEE, 2021*, 1–4.
30. Mo, X., & Xu, J. (2021). Energy-efficient federated edge learning with joint communication and computation design. *Journal of Communications and Information Networks, 6*(2), 110–124.
31. Abd-Elnaby, M., Sedhom, G. G., El-Rabaie, E.-S.M., & Elwekeil, M. (2022). An optimum weighted energy efficiency approach for low complexity power allocation in downlink NOMA. *IEEE Access, 10*, 80667–80679.
32. Islam, D. M. S., Das, N., Uddin, M. F. (2022). Energy efficiency analysis of FSO backhauled uplink noma system. In: *2022 25th International Conference on Computer and Information Technology (ICCIT)*. IEEE, pp. 159–163.
33. Katwe, M., Singh, K., Sharma, P. K., & Li, C.-P. (2021). Energy efficiency maximization for UAV-assisted full-duplex NOMA system: User clustering and resource allocation. *IEEE Transactions on Green Communications and Networking, 6*(2), 992–1008.
34. Mahady, I. A., Bedeer, E., Ikki, S., & Yanikomeroglu, H. (2022). Energy efficiency maximization of full-duplex NOMA systems with improper gaussian signaling under imperfect self-interference cancellation. *IEEE Communications Letters, 26*(7), 1613–1617.
35. Thi, H. N., Kieu, T. X., Truong, L. H., & Le Thi, A. (2023). Resource allocation for noma, IRS network with energy harvesting in presence of hardware impairment. In: IEEE 3rd International Conference in Power Engineering Applications (ICPEA). *IEEE,* Vol. 2023, pp. 169–174.
36. Kumar, M. H., Sharma, S., Deka, K., & Thottappan, M. (2022). Reconfigurable intelligent surfaces assisted hybrid NOMA system. *IEEE Communications Letters, 27*(1), 357–361.
37. Cao, S., & Hou, F. (2022). On the maximum energy efficiency of random access-based OMA and NOMA in multirate environment. *IEEE Transactions on Wireless Communications, 21*(12), 10438–10454.
38. Venkatesh, T., & Chakravarthi, R. (2022). An energy efficient algorithm in manet using monarch butterfly optimization and cluster head load distribution. In: *2022 International Conference on Communication, Computing and Internet of Things (IC3IoT)*. IEEE, pp. 1–5.
39. Prasad, L. C., Kamatham, Y., & Sunehra, D. (2022). An energy efficient clustering and relay selection scheme for cognitive radio sensor networks. In: *2022 International Conference on Innovations in Science and Technology for Sustainable Development (ICISTSD)*. IEEE, pp. 30–35.
40. Alhashimi, H. F., Hindia, M. N., Dimyati, K., Hanafi, E. B., Safie, N., Qamar, F., Azrin, K., & Nguyen, Q. N. (2023). A survey on resource management for 6g heterogeneous networks: Current research, future trends, and challenges. *Electronics, 12*(3), 647.
41. Puspitasari, A. A., An, T. T., Alsharif, M. H., & Lee, B. M. (2023). Emerging technologies for 6G communication networks: Machine learning approaches. *Sensors, 23*(18), 7709.
42. Goldsmith, A. (2005). *Wireless communications*. Cambridge university press.
43. Khan, H. Z., Ali, M., Naeem, M., Rashid, I., Siddiqui, A. M., Imran, M., & Mumtaz, S. (2020). Joint admission control, cell association, power allocation and throughput maximization in decoupled 5g heterogeneous networks. *Telecommunication Systems*, pp. 1–14.
44. Ali, Z. J., Noordin, N. K., Sali, A., Hashim, F., & Balfaqih, M. (2020). Novel resource allocation techniques for downlink non-orthogonal multiple access systems. *Applied Sciences, 10*(17), 5892.
45. Rajoria, S., Trivedi, A., & Godfrey, W. W. (2021). Sum-rate optimization for NOMA based two-tier hetnets with massive MIMO enabled wireless backhauling. *AEU-International Journal of Electronics and Communications, 132*, 153626.
46. Saito, Y., Kishiyama, Y., Benjebbour, A., Nakamura, T., Li, A., & Higuchi, K. (2013). Non-orthogonal multiple access (noma) for cellular future radio access. In: IEEE 77th vehicular technology conference (VTC Spring). *IEEE,* Vol. 2013, pp. 1–5.
47. Moltafet, M., Azmi, P., Mokari, N., Javan, M. R., & Mokdad, A. (2018). Optimal and fair energy efficient resource allocation for energy harvesting-enabled-PD-NOMA-based hetnets. *IEEE Transactions on Wireless Communications, 17*(3), 2054–2067.
48. Tomida, S., & Higuchi, K. (2011). Non-orthogonal access with sic in cellular downlink for user fairness enhancement. In: International symposium on intelligent signal processing and communications systems (ISPACS). *IEEE,* Vol. 2011, pp. 1–6.
49. Xie, H., & Xu, Y. (2022). Robust resource allocation for NOMA-assisted heterogeneous networks. *Digital Communications and Networks, 8*(2), 208–214.
50. Han, T., Gong, J., Liu, X., Islam, S.R., Li, Q., Bai, Z., & Kwak, K. S. (2018). On downlink noma in heterogeneous networks with non-uniform small cell deployment. *IEEE Access*, Vol. 6, pp. 31 099–31 109.

51. Fletcher, R., & Leyffer, S. (1994). Solving mixed integer nonlinear programs by outer approximation. *Mathematical programming, 66*(1–3), 327–349.
52. Duran, M. A., & Grossmann, I. E. (1986). An outer-approximation algorithm for a class of mixed-integer nonlinear programs. *Mathematical programming, 36*, 307–339.
53. Khan, H. Z., Ali, M., Naeem, M., Rashid, I., Siddiqui, A. M., Imran, M., & Mumtaz, S. (2020). Resource allocation and throughput maximization in decoupled 5G. In: IEEE wireless communications and networking conference (wcnc). *IEEE,* Vol. 2020, pp. 1–6.
54. Floudas, C. A. & Pardalos, P. M. (2008). *Encyclopedia of optimization*. Springer Science & Business Media.
55. Pistikopoulos, E. N. (1998). Ca floudas, nonlinear and mixed-integer optimization. fundamentals and applications.
56. Land, A. H. & Doig, A. G. (2010). *An automatic method for solving discrete programming problems*. Springer.
57. Bonami, P. (2011). Lift-and-project cuts for mixed integer convex programs. In: Integer Programming and Combinatoral Optimization: 15th International Conference, IPCO. (2011). New York, NY, USA, June 15–17, Proceedings 15. *Springer, 2011*, 52–64.
58. Bharany, S., Sharma, S., Alsharabi, N., Tag Eldin, E., & Ghamry, N. A. (2023). Energy-efficient clustering protocol for underwater wireless sensor networks using optimized glowworm swarm optimization. *Frontiers in Marine Science, 10*, 1117787.
59. Kulmar, M., Müürsepp, I., & Alam, M. M. (2023). Heuristic radio access network subslicing with user clustering and bandwidth subpartitioning. *Sensors, 23*(10), 4613.
60. Taneja, A., Saluja, N., Taneja, N., Alqahtani, A., Elmagzoub, M., Shaikh, A., & Koundal, D. (2022). Power optimization model for energy sustainability in 6g wireless networks. *Sustainability, 14*(12), 7310.
61. Beitollahi, M., & Lu, N. (2022). Multi-frame scheduling for federated learning over energy-efficient 6g wireless networks. In: *IEEE INFOCOM 2022-IEEE Conference on Computer Communications Workshops (INFOCOM WKSHPS)*. IEEE, pp. 1–6.
62. Imoize, A. L., Obakhena, H. I., Anyasi, F. I., & Sur, S. N. (2022). A review of energy efficiency and power control schemes in ultra-dense cell-free massive MIMO systems for sustainable 6G wireless communication. *Sustainability, 14*(17), 11100.
63. Nurcahyani, I., & Lee, J. W. (2021). Role of machine learning in resource allocation strategy over vehicular networks: A survey. *Sensors, 21*(19), 6542.
64. Fernando, X., & Lăzăroiu, G. (2023). Spectrum sensing, clustering algorithms, and energy-harvesting technology for cognitive-radio-based internet-of-things networks. *Sensors, 23*(18), 7792.
65. Mohsan, S. A. H., Othman, N. Q. H., Li, Y., Alsharif, M. H., & Khan, M. A. (2023). Unmanned aerial vehicles (UAVS): Practical aspects, applications, open challenges, security issues, and future trends. *Intelligent Service Robotics, 16*(1), 109–137.
66. Arafat, M. Y., Alam, M. M., & Moh, S. (2023). Vision-based navigation techniques for unmanned aerial vehicles: Review and challenges. *Drones, 7*(2), 89.
67. Zear, A., & Ranga, V. (2022). UAVS assisted network partition detection and connectivity restoration in wireless sensor and actor networks. *Ad Hoc Networks, 130*, 102823.
68. Charnes, A., & Cooper, W. W. (1962). Programming with linear fractional functionals. *Naval Research Logistics Quarterly, 9*(3–4), 181–186.

Umar Ghafoor received the MS Electrical Engineering degree from National University of Sciences and Technology, Pakistan with a major in wireless communication. He has been associated with the profession of teaching and research since 2013. His research interests include wireless communication, resource allocation, optimization theory, heterogeneous networks, cognitive radio networks.

Tahreem Ashraf received the MPhil degree from Government College University, Faisalabad Pakistan with a major in Pure Math. She has been associated with the profession of teaching and research since 2018. Her research interests include optimization theory, graph theory and linear algebra.